THE UNIVERSITY OF CALGARY

DIGITAL ANGULAR SPEED MEASUREMENT OF A GENERATING UNIT USING WAVEFORM SAMPLING

by

JEREMY JAMES

A THESIS

SUBMITTED TO THE FACULTY OF GRADUATE STUDIES

IN PARTIAL FULFILMENT OF THE REQUIREMENTS FOR THE DEGREE

OF MASTER OF SCIENCE

DEPARTMENT OF ELECTRICAL ENGINEERING

CALGARY, ALBERTA

JUNE, 1978

THE UNIVERSITY OF CALGARY

FACULTY OF GRADUATE STUDIES

The undersigned certify that they have read, and recommend to the Faculty of Graduate Studies for acceptance, a thesis entitled, "Digital Angular Speed Measurement of a Generating Unit using Waveform Sampling", submitted by Jeremy James in partial fulfillment of the requirements for the degree of Master of Science.

Dr. O.P. Malik
Chairman - Examining Committee
Electrical Engineering

Dr. G.S. Hope
Electrical Engineering

Dr. S.T. Nichols
Electrical Engineering

Dr. P.R. Bishnoi
Chemical Engineering

Date May 31, 1978

ABSTRACT

In this thesis a new method of digital angular speed measurement is proposed. A method of waveform sampling utilizing an orthogonal pair of sinusoids is developed. Earlier techniques of speed measurement are discussed and two forms of the most promising technique are analyzed. One of these forms is compared with the proposed waveform sampling technique by estimating the speed of a turbine-generator unit model under steady state and transient conditions.

The results of the steady state and transient tests are presented. Under steady state conditions the waveform sampling technique was found to have a resolution of 0.05 Hz on a 60 Hz base that is updated approximately once every 1.25 ms. Transient studies showed that the waveform sampling technique responds well to a change in speed, but the resolution decreases to 2%. Recommendations that should improve the performance are made and a discussion of a practical implementation of the waveform sampling method to the speed measurement problem is presented.

ACKNOWLEDGEMENTS

The author wishes to express his appreciation to Dr. O. P. Malik, Dr. G. S. Hope, and the weekly colloquy for guidance during this investigation. A special thanks to Dr. O. P. Malik for his advice and assistance during preparation of the manuscript.

Technical advice from Mr. R. A. Peters, Mr. B. Hriskevich, Mr. P. Walsh and Mr. J. Geerligs is acknowledged with thanks.

The author is grateful to the National Research Council for funding received for this project.

Special thanks are due to Miss F. Fernandes for her encouragement.

TO MY

PARENTS, BROTHER AND FRIENDS

TABLE OF CONTENTS

TABLE OF CONTENTS (CONT'D)

TABLE OF CONTENTS (CONT'D)

LIST OF TABLES

LIST OF FIGURES

LIST OF FIGURES (CONT'D)

LIST OF FIGURES (CONT'D)

LIST OF SYMBOLS

t	time
$x(t)$	analog signal
$h(t)$	impulse response
$p_T(t)$	rectangle pulse T seconds long
f	frequency
$H(f)$	Fourier transform of impulse response
f_1	unknown frequency that is estimated
f_s	sampling frequency
T	constant time interval
T_s	sampling rate
kT	kth time interval
$x(kT)$	sample at kth time interval
$x_Q(kT)$	quantized sample at kth time interval
$e(kT)$	quantization error at kth time interval
$x_T(kT_s)$	sample at the kth time interval of a finite length sequence
$w(kT)$	a weight at the kth time interval
$X(e^{j2\pi f})$	Fourier transform of a discrete time sequence
$X_{i,T}(e^{j2\pi f})$	i odd, real part of Fourier transform i even, imaginary part of Fourier transform
N	number of weights
$E(N,T_s,f_1,f)$	estimate of f_1
$\hat{}$	denotes an orthogonal signal
A	amplitude

ε	error in amplitude
B	resolution of E
Φ	air gap flux
K	coefficient representing the number of conductors and the winding of an armature
Δ	quantization level
P(e)	probability density function
n	mean error
σ^2	variance
τ	dummy variable of time
j	complex operator
ψ	phase angle
ZOH	zero-order hold

CHAPTER 1

INTRODUCTION

1.1 BACKGROUND

An electric power system is composed of some or all of the four major components: generation, transmission, distribution and load.[1] Generation is the conversion of energy from a readily available form to electric energy. Transmission enables the energy in the electrical form to be transported in bulk from a generation centre to a load centre. Distribution is the division of energy to meet the demand of individual loads at the load centre. The destination of electric energy is the device where it is converted to another form suitable to the task at hand. This is the load or consumer which may be a factory, office building, home, etc.

Each individual power system is not identical. For example, the generation may be located at the load centre. This minimizes the need for transmission, because the total generation will immediately be distributed to the loads. Alternatively, the demand at a generation site could be large enough to require all the generation. This could exist at a large industrial complex and in this case the distribution is localized. In general, power systems consist of some or all of the major components. Thus, independent of the application, individual power systems have similar composition.

On a scale larger than the individual power system, another component arises which is of equal importance with those discussed above. This is the electrical interconnections that exist when power systems are grouped to form power pools. Power pools originated from a need to reduce the cost of an electric energy system by sharing generation and loads on a contractual basis.[2] Also, the security of electricity supply to the consumers in a power pool is greater in emergency situations such as those resulting from faults or loss of transmission. However, interconnecting the systems introduces additional problems. The stability of the system is now more sensitive to disturbances so more sophisticated control is required.

1.2 STABILITY OF THE POWER SYSTEM

A common definition of the stability of a power system is the ability of the individual sections of the system to operate in step with the rest of the system, that is, to maintain synchronism. This means that all generators in the system generate electric energy at the same frequency independent of changes in demand.

Power produced by a generating unit is directly proportional to the product of the rotor torque and its speed. The electric frequency of the current and the voltage generated is directly proportional to the rotational speed. To maintain synchronism while the demand changes requires that the torque and speed of each generator should change such that the product of new torque and speed meets the new demand and keeps the speed of all the generators in the interconnected system the same. If this occurred the system frequency would change proportionately and the system would remain stable. However, because of other

considerations, the frequency must be maintained at one value.[2] Therefore, changing demands on a power system must be satisfied by changing the torque only. This is the ideal solution as explained below.

Loads in a power system are supplied from a specific generation centre or by generation centres. When the load demand increases, it must be matched by increased generation. At the generation centre concerned the speed of the generators decreases because energy is extracted from the rotating shafts. Unless increased torque is applied, the speed will remain low. Thus, the generator will operate at an asynchronous speed with respect to the rest of the system, and an unstable situation will exist. The conclusion of the previous paragraph was that the torque should be increased instead of allowing the speed to change. How, the question arises, is the operator to know that a different demand exists? A solution is that he monitor the speed of the generator. So to ensure system stability and maintain synchronism, the speed of the generators in the system should be observed for an indication of change in demand.

1.3 OBJECTIVES AND SCOPE OF THIS THESIS

As stated previously, one of the reasons for interconnecting power systems to form power pools is to share the loads. With the increase in load being unmatched by an increase in generation capacity, power systems are fast approaching their stability limit. This is evident from literature by the increase in required frequency resolution over the last ten years. The increase in resolution has been fivefold, from 0.083% to 0.017%.[2,3] So to insure system stability, a technique that measures generator speed to a high degree of resolution is required.

The objective of this thesis is to build a speed transducer with a resolution of 0.017%. For reasons stated in the next paragraph, this transducer will be implemented digitally and will be required to update the speed estimate every 20 milliseconds.

Previous authors have established that a machine model of a generating unit can be controlled automatically using on-line digital controllers operating in real-time. This is known as direct digital control.[4,5,6] The work described in this thesis relates to the design of a digital angular speed transducer for use in the direct digital control of the above-mentioned machine model. To the best of the author's knowledge, the theoretical approach used in this thesis has previously not been employed to the problem of measuring speed. The outcome of the work is a method of measuring speed digitally that can be implemented easily. It employs a method of asynchronous waveform sampling which eliminates errors when the truncation interval is not equal to the period of the sampled waveform.

A survey of the digital techniques proposed earlier and an analysis of these methods is given in Chapter 2. Chapter 3 discusses the theoretical background of the technique proposed by the author. A practical implementation and the specification of the sampling rate, data window length and the resolution are discussed in Chapter 4. The results of static and transient tests performed on the proposed technique and one of the recent techniques are described in Chapter 5. Chapter 6 states the conclusions and gives a general discussion of the thesis. The pros and cons of the tested techniques are discussed and recommendations are made for further work.

CHAPTER 2

PRESENT DIGITAL ANGULAR SPEED MEASUREMENT TECHNIQUES

2.1 INTRODUCTION

It is expected that in the foreseeable future, control of electric power generation will be implemented in an entirely digital form. A requirement of this method is that the information needed to determine the control must be represented digitally. Angular speed measurement for application in the direct digital control of a turbine-generator is the case in point.

Digital angular speed measurement techniques have been reported previously. The most promising methods for application to direct digital control are those that use slotted discs rigidly attached to the rotor shaft of a turbine-generator.[7-12] The rotational displacement of the shaft is encoded as an integral number by the disc, and a logic circuit[7,9,10] or software algorithm[8,11,12] will produce a velocity estimate. One type counts the number of slots that pass by a fixed point in a fixed time period and is designated as a constant-time speed resolver.[7-9] The second type is designated as a constant-displacement speed resolver, because angular velocity is estimated by measuring the time for a fixed rotational displacement.[10-12] The slotted disc used in these measurements is known as a shaft-encoder and has been used in shaft positioning applications such as those in steel mills, pulp and

paper mills and radar tracking systems.[13] Reported resolution of these techniques is 0.003% to 0.2% updated from 33 to 1 ms.[10-12]

A technique similar to that mentioned above uses a microwave Doppler transceiver to sense a specific anomaly on the rotor shaft as a means of measuring displacement.[14] This method reports a resolution of 0.05% updated once every 66 ms.

The phase lock loop principle has been applied to both the digital measurement of electric frequency and angular velocity.[15,16] In this technique speed estimates are updated every 100 ms.

The purpose of this thesis is to develop a digital angular speed transducer which has a resolution of 0.017% and updates every 25 ms. In this chapter, techniques which have similar performance are analyzed so that the speed measurement method proposed may be compared with methods reported earlier. Of the methods discussed above only the two shaft-encoder techniques have comparable specifications; therefore only these will be analyzed. Topics studied are: errors introduced by quantization and nonideal effects resulting from the approximation used to estimate the angular velocity.

2.2 SHAFT-ENCODER QUANTIZATION

Constant-time and constant-displacement resolvers are similar in construction, so the method used to analyze one is applicable to the other. However, the errors inherent in the encoding processes used are different in nature for each resolver. A typical application of these techniques is depicted in Fig. 2.1.

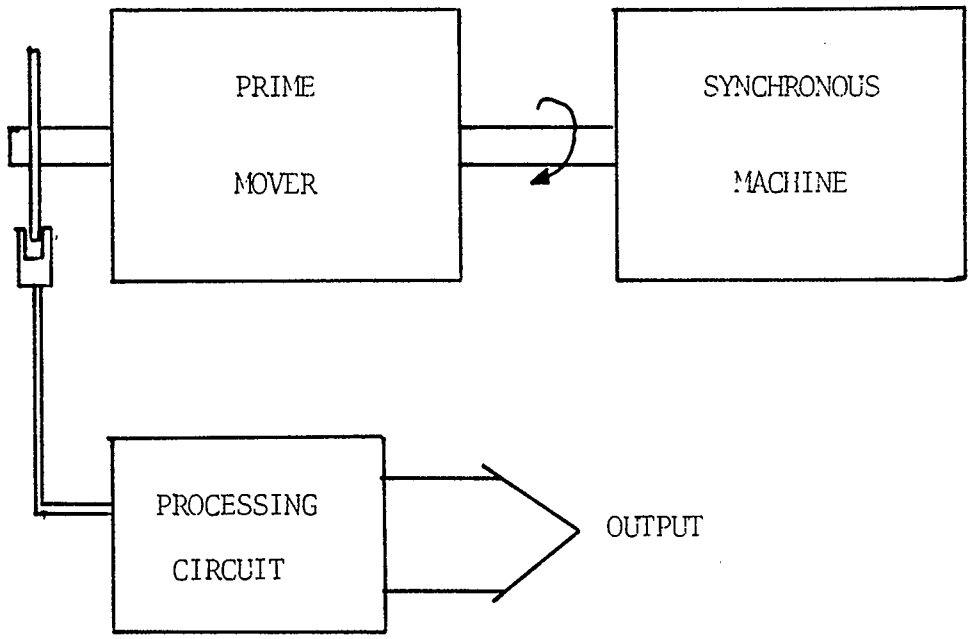

Fig. 2.1 Digital angular speed measurement using a shaft-encoder.

2.2.1 Constant-Time Speed Resolvers

A process similar to shaft-encoding with slotted discs is analog to digital (A/D) conversion. Fig. 2.2 is a simple block diagram of an A/D converter. The input to the converter, x(t), is an analog signal that is sequentially sampled by the sample/hold block. Sampled data x(kT) is converted to a binary number, $x_Q(kT)$, by the quantizer block. If this is an N bit A/D converter, the quantizer will encode the sampled signal as a number in the range 0 to 2^N-1. There are only a finite number of values for $x_Q(kT)$ to represent the infinite possible values

of x(kT). Therefore, $x_Q(kT)$ is an approximation of x(kT). The approximating or quantizing of x(kT) introduces the quantization error defined below:

$$e(kT) = x(kT) - x_Q(kT). \tag{2.1}$$

Quantization similar to this occurs when angular displacement is represented by an integer number of slots, like those used by the shaft-encoder scheme depicted in Fig. 2.1.

If a shaft-encoder is used to measure angular velocity, then the angular displacement of a rotating shaft is measured by sensing the number of slots rotating past a sensor in a given time period. Given

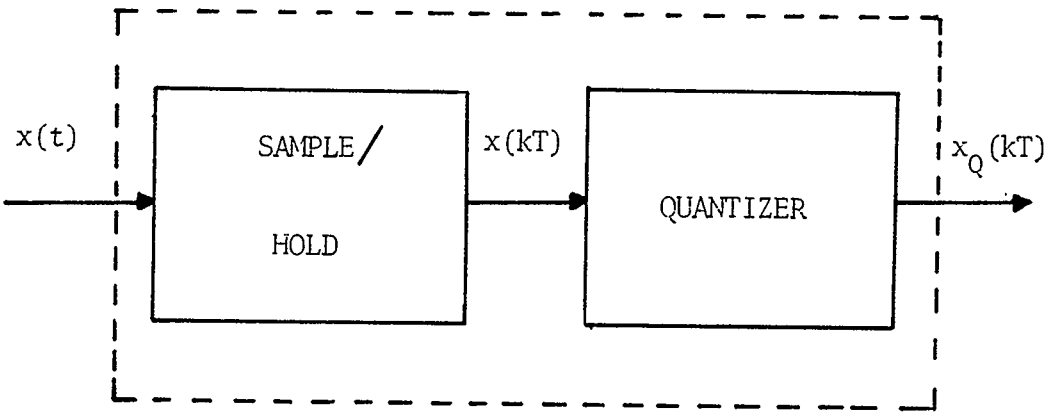

Fig. 2.2 Analog to digital converter

that there are N slots uniformly spaced around the perimeter of the encoder, then the minimum detectable angular displacement is $2\pi/N$ radians. Fig. 2.3 relates the quantized angular displacement $x_Q(kT)$ to the real angular displacement $x(t)$. This graph is called a quantization characteristic. It represents the quantization that results from shaft-encoding. In this figure the horizontal axis is the physical value of rotation and the vertical axis is the quantized rotation after encoding. Rotation greater than 0 radians and less than or equal to $2\pi/N$ radians is quantized to 0 radians and rotation greater than $2\pi/N$ radians and less than $4\pi/N$ radians is quantized to $2\pi/N$ radians and so on.

There are three kinds of quantization: roundoff, truncation and sign magnitude truncation. Fig. 2.3 is representative of quantization with truncation, because the data $x_Q(kT)$ is the highest quantization level that is less than the real signal.[17] The error in the quantized signal shown in Fig. 2.3 is defined by the limits,

$$0 \leq e(kT) < \Delta \tag{2.2}$$

where

$$\Delta = 2\pi/N. \tag{2.3}$$

The probability density function, $P(e)$, of this error is uniform and is illustrated by Fig. 2.4.[17,18] The expected or mean value of the error is,

$$\eta = E[e(kT)] = \int_{-\infty}^{\infty} e(kT)P[e(kT)]de(kT); \tag{2.4}$$

therefore

$$\eta = \pi/N, \tag{2.5}$$

and the variance of the mean error is,[19]

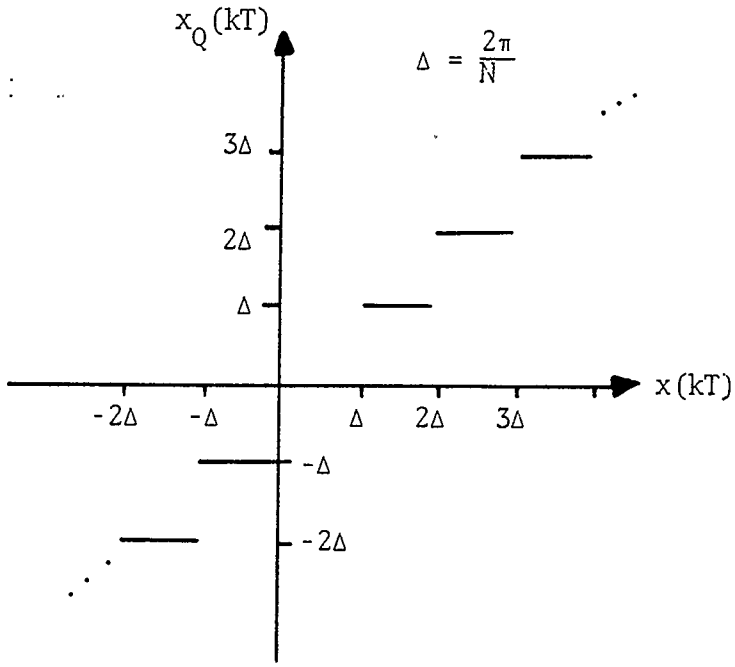

Fig. 2.3 Shaft-encoder quantization characteristic.

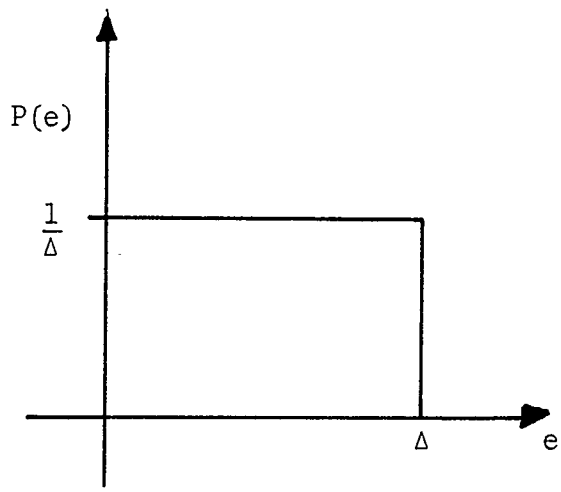

Fig. 2.4 Probability density function of shaft-encoder quantization error.

$$\sigma^2 = E\,[e(kT)-\eta]^2 = \int_{-\infty}^{\infty} [e(kT)-\eta]^2 P[e(kT)]\,de(kT) \qquad (2.6)$$

$$\sigma^2 = (2\pi/N)^2\ 1/12. \qquad (2.7)$$

From eqn. (2.5) the mean of the quantization error varies inversely with the number of slots and from eqn. (2.7) the variance varies inversely with the square of the number of slots. So doubling the number of slots on the encoder will half the mean error and divide the variance of the mean error by four. This technique estimates angular velocity by producing a weighted value of angular displacement. Therefore, if a velocity resolution of 0.017% is required, the estimate of displacement must be resolvable to 0.017% of 2π radians or about 1.068×10^{-3} radians. Letting this equal the mean error, the minimum number of slots required as calculated by eqn. (2.5) is 2942.

2.2.2 Constant-Displacement Resolvers

Constant-displacement resolvers measure the time taken for the rotor to rotate a specific angular displacement. The shaft-encoder does not introduce error because the angular displacement is always the same. However, clock pulses are counted instead of slots. Therefore, time rather than displacement is quantized.

Accurate time bases are available today, so errors in the pulse rate can be considered negligible. The counting sequence is started and stopped by a slot on the encoder passing a fixed point. Therefore the time measurement of the displacement is the count reached before the sequence is stopped. Again this is truncation and the quantization characteristic of Fig. 2.3 applies. The quantization level, Δ, is

equal to $1/f_s$ where f_s is the clock frequency. Therefore, the same derivation used to calculate eqns. (2.5) and (2.7) can be used by replacing Δ with $1/f_s$. So from eqns. (2.4) and (2.6) the mean error and variance of the mean error of the time quantization are:

$$\eta = 1/2f_s \tag{2.8}$$

$$\sigma^2 = \frac{1}{12(f_s)^2} \tag{2.9}$$

The mean of the quantization error varies inversely with the clock frequency and the variance varies inversely with the square of the clock frequency. For the required resolution in velocity as before and at an angular speed of 1800 rpm, the resolution in the time measurement is required to be about 5.6 microseconds. Therefore, using eqn. (2.8), the clock frequency required is about 89 kHz if one slot on the disc is used. For two slots placed directly opposite each other on the encoding disc, a clock rate twice this frequency is required.

2.3 FREQUENCY ANALYSIS OF SHAFT-ENCODED ANGULAR SPEED RESOLVERS

The previous section demonstrated that the signal from a shaft-encoder has an error due to quantization of either the time or the displacement variable. This section shows how data from the encoder is used to generate a speed estimate. The method can be described as a zero-order approximation. Analysis of this approximation is accomplished by assuming that the encoding device has infinite resolution. If it does, then the quantization effects that have been discussed do not occur and all nonideal results that do occur come from the zero-order approximation that is used. This allows a separate analysis of the effects of quantization and of zero-order approximation.

An estimate of angular velocity is made at the end of each measurement period. This represents the velocity of the shaft until a new estimate, independent of all those made previously, replaces the old estimate. This can be described as taking the first term of the power series expansion of x(t) on the interval kT to (k+1)T given by,

$$x_k(t) = x(kT) + x'(kT)(t-kT) + x''(kT)(t-kT)^2/2! + \ldots \quad (2.10)$$

where the single prime (') is the first derivative with respect to time and T is the time between estimates. The estimate at the k^{th} interval is $x_k(t)$ as shown by

$$x_k(t) = x(kT). \quad (2.11)$$

This equation shows that the estimate is dependent upon only the present sample. All previous samples have no effect.

In eqn. (2.11) T has two interpretations. For a constant-time shaft-encoder, T is the time period over which pulses from the encoder are counted. In this case T is always the same. But for a constant-displacement shaft-encoder, T depends on the angular velocity of the shaft. Hence it is a variable. Effects of these two interpretations of T are discussed in the following paragraphs.

A hypothetical device that is defined by eqn. (2.11) is known as a zero-order hold (ZOH). Fig. 2.5 is a block diagram describing a ZOH. To understand the nature of this device its transfer function must be derived. The transfer function of a linear system is the Fourier Transform (FT) of the time domain impulse response function.[20] The impulse response measured at the output of the summer in Fig. 2.5 is

$$h(t) = \delta(t) - \delta(t-T). \quad (2.12)$$

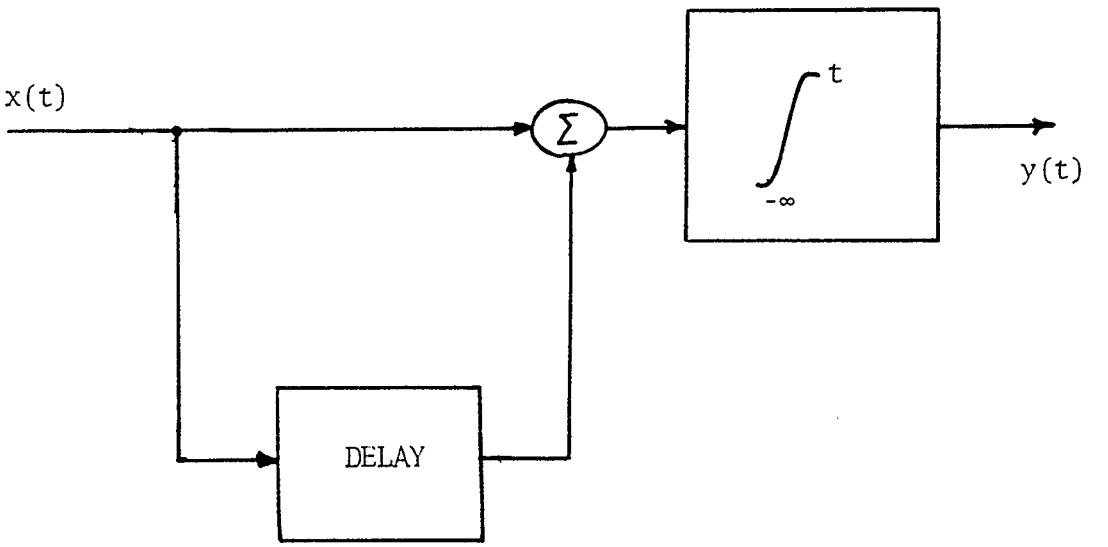

Fig. 2.5 Block diagram of a zero-order hold.

Therefore, the impulse response of the ZOH is the integral of eqn. (2.12) and is defined as $h_{ZOH}(t)$ in eqn. (2.13). Thus,

$$h_{ZOH}(t) = \int_{-\infty}^{t} [\delta(\tau)-\delta(\tau-T)]d\tau \qquad (2.13)$$

or

$$h_{ZOH}(t) = \begin{cases} 1 & 0 \leq t < T \\ 0 & \text{elsewhere} \end{cases} \qquad (2.14)$$

The FT of eqn. (2.14) is the desired transfer function. This is defined by eqn. (2.15) below:

$$H_{ZOH}(f) = \int_{-\infty}^{\infty} h_{ZOH}(t)\, e^{-j2\pi ft}\, dt \qquad (2.15)$$

$$\text{or} \qquad H_{ZOH}(f) = \frac{T\sin(\pi fT)}{\pi fT} e^{-j\pi fT}. \tag{2.16}$$

Fig. 2.6 illustrates the magnitude of the amplitude response of the zero-order hold.

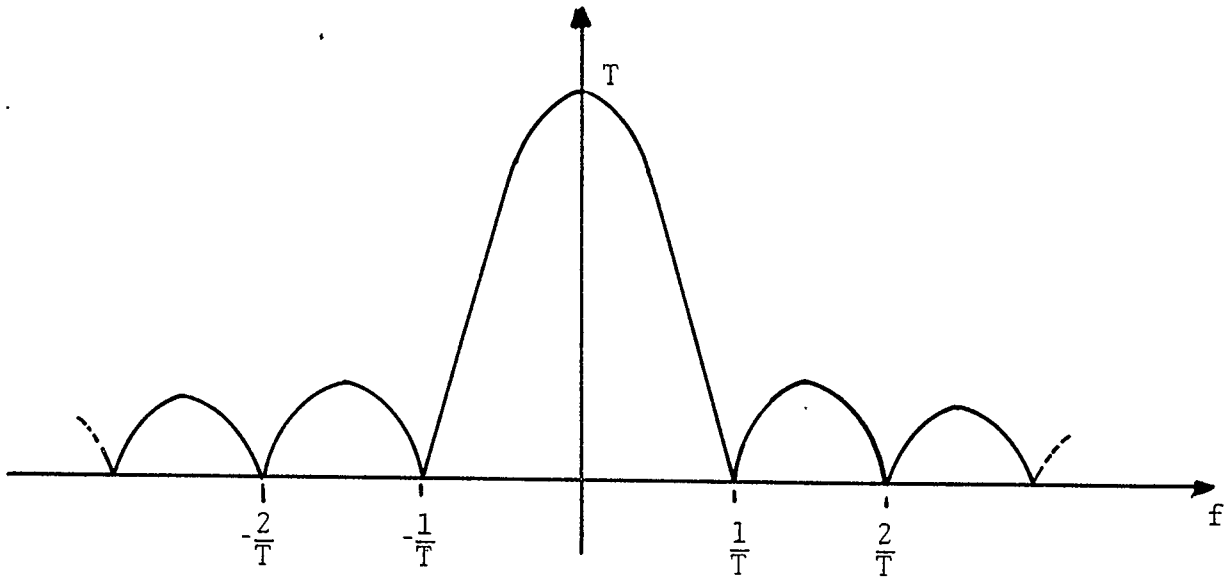

Fig. 2.6 Amplitude response of zero-order hold.

If the signal input to the ZOH is a constant value, this technique will determine the input exactly, but if the input is time varying then the ZOH will estimate the input incorrectly. Error introduced can be found from Fig. 2.6. A constant signal results in the output being weighted with T. If the signal has an oscillating component, then the estimate of this component is weighted by $H_{ZOH}(f)$ evaluated at f equal to the frequency at which this component oscillates. An extreme case

occurs if the input signal has a sinusoidal component at frequency 1/T. If this occurs then the ZOH will completely eliminate this component from the estimate leaving only the constant or "dc" level of the original signal.

This analysis applies to constant-time speed resolvers. Analysis of the constant-displacement resolver will give the same result. But the difference between the techniques is that the sampling interval for the latter depends upon the angular speed of the rotor shaft. If the shaft speed is constant, then the estimate of the speed is given by T. However, the same oscillation in the shaft speed will be estimated differently if the average or dc value of the speed changes. Because the amplitude of this oscillation is a function of T as given by eqn. (2.16).

2.4 CONCLUSION

Constant-time and constant-displacement speed resolvers have been analyzed for errors produced by shaft-encoder quantization, time quantization and zero-order hold approximation. Constant-time resolvers require a minimum of 2942 slots to achieve ±0.017% velocity resolution. Error introduced by zero-order hold approximation is illustrated in Fig. 2.6.

Constant displacement-resolvers exhibit a time quantization error that results from counting pulses from a clock to measure rotation. This sets a lower limit on the frequency of the clock rate used to measure displacement. If one slot is used the minimum clock rate is 89 kHz. Error from the approximation used to estimate angular speed is speed dependent and can be calculated from Fig. 2.6 with the knowledge that T, in this case, is time varying.

CHAPTER 3

PROPOSED DIGITAL ANGULAR SPEED MEASUREMENT TECHNIQUE

3.1 INTRODUCTION

A technique to measure the frequency of a sinusoidal signal is discussed in this chapter. This is a digital method that uses a block of data to calculate a frequency estimate. The block is formed by truncating the sequence of data that are samples of the periodic signal.

Truncation in time results in a "smearing" of the frequency domain representation of the signal.[21] This is shown by studying frequency spectrums of infinite length and finite length data sequences. A result of the smearing effect is used to develop the proposed frequency measurement technique. The technique is similar to the Fourier Transform (FT) in that a frequency estimate is produced by weighting the sampled data with samples of a sinusoidal reference.

3.2 TRUNCATION OF DISCRETE TIME SIGNALS

An algorithm that processes sampled data can perform operations only on a finite length data block. If the data are samples of a continuous signal, then formation of a data block requires the truncation of the discrete time sequence. After truncation the data samples form a finite length sequence, which is the only modification from a time domain point of view. However, the frequency domain representation of the truncated sequence is different from that of the infinite length

sequence. Therefore, time domain truncation of an infinite length sequence will be studied from the frequency domain point of view.

Eqn. (3.1) defines a continuous sinusoidal signal at frequency f_1 Hz and initial phase of ψ radians:

$$x(t) = \cos(2\pi f_1 t + \psi). \tag{3.1}$$

Let this signal be sampled at f_s Hz. Then the sampled signal is

$$x(kT_s) = \cos(2\pi f_1 kT_s + \psi), \quad -\infty < k < \infty, \tag{3.2}$$

where T_s is the sampling rate. A data sample is found by evaluating $x(kT_s)$ at a value of k in the limit shown. Eqn. (3.2) is an infinite length discrete time sequence. This sequence may be described in the frequency domain by applying the FT defined by eqn. (3.3).[17]

$$X(e^{j2\pi fT_s}) = \sum_{k=-\infty}^{\infty} x(kT_s)e^{-j2\pi fkT_s}. \tag{3.3}$$

The magnitude of the FT of eqn. (3.2) is illustrated in Fig. 3.1(a). This is a pair of impulses centred around zero Hz (dc) and at integer multiples of the sampling frequency.

A data block N samples long is formed by taking N consecutive values of eqn. (3.2). This finite length data block is a truncated form of the infinite length sequence. Truncation is equivalent to multiplying eqn. (3.2) by the function defined by

$$p_T(kT_s) = \begin{cases} 1 & 0 \le k < N, \quad T = NT_s \\ 0 & \text{elsewhere} \end{cases} \tag{3.4a}$$

where T is the length of the truncation interval. This product is

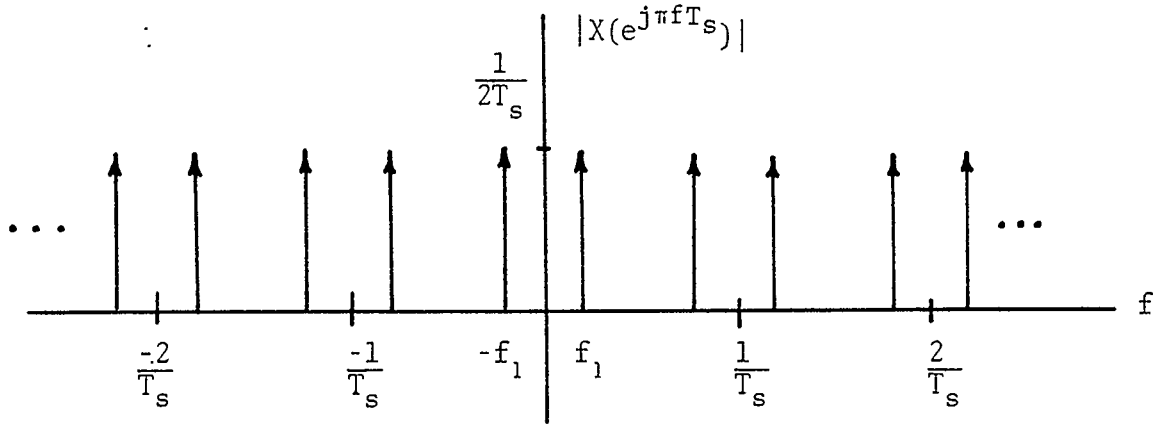

Fig. 3.1(a) Fourier transform of eqn. (3.2).

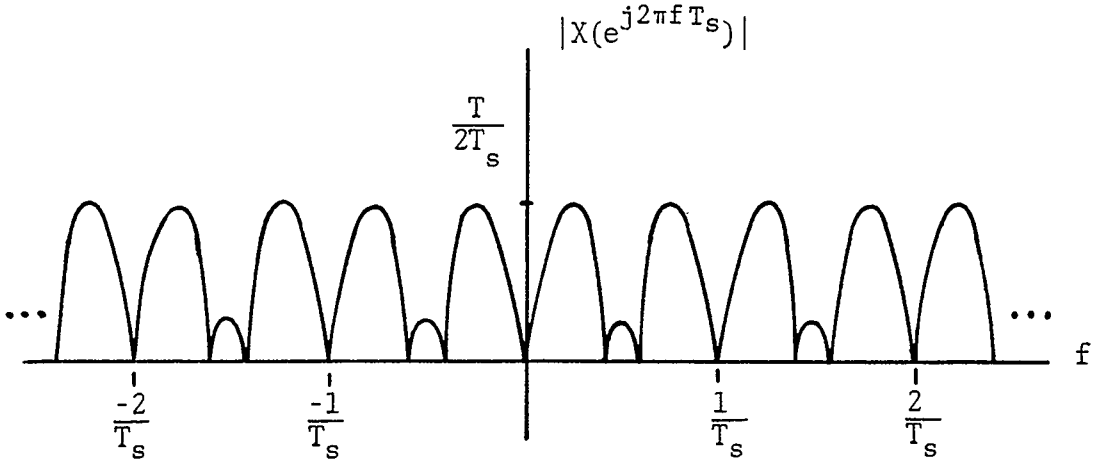

Fig. 3.1(b) Illustration of eqn. (3.9).

derived by

$$x_T(kT_s) = x(kT_s)\ p_T(kT_s) \tag{3.4b}$$

and the result is given by eqn. (3.5), which describes N consecutive samples of x(t) in the limit shown:

$$x_T(kT_s) = cos(2\pi f_1 kT_s + \psi), \quad 0 \le k < N. \tag{3.5}$$

For k outside this limit the product is equal to zero. Therefore, eqn. (3.5) is a truncated signal.

The FT of eqn. (3.5) is evaluated below to find the frequency domain representation of the truncated signal:

$$X_T(e^{j2\pi fT_s}) = \sum_{k=-\infty}^{\infty} x_T(kT_s)e^{-j2\pi fkT_s}. \tag{3.6}$$

Since eqn. (3.5) is zero outside the limits shown

$$X_T(e^{j2\pi fT_s}) = \sum_{k=0}^{N-1} cos(2\pi f_1 kT + \psi)\ e^{-j2\pi fkT_s}. \tag{3.7}$$

Appendix I describes the mechanics of deriving the closed form equivalent of eqn. (3.7), which is given below:

$$X_T(e^{j2\pi fT_s}) = \frac{e^{j\pi fT_s(N-1)}}{2}\left[e^{-j(\pi f_1 T_s(N-1)+\psi)}\ \frac{sin(NT_s\pi(f_1+f))}{sin(T_s\pi(f_1+f))}\right.$$

$$\left. + e^{j(\pi f_1 T_s(N-1)+\psi)}\ \frac{sin(NT_s\pi(f_1-f))}{sin(T_s\pi(f_1-f))}\right]. \tag{3.8}$$

If the sampling frequency is an integer multiple of the frequency of x(t), then the magnitude of eqn. (3.8) is as given below:

$$|X_T(e^{j2\pi fT_s})| = \frac{1}{2}\left[\frac{sin^2 N\pi T_s(f_1+f)}{sin^2\pi T_s(f_1+f)} + \frac{sin^2 N\pi T_s(f_1-f)}{sin^2\pi T_s(f_1-f)} + 2\,\frac{sin N\pi T_s(f_1+f)}{sin\pi T_s(f_1+f)}\right.$$

$$\left.\times\,\frac{sin N\pi T_s(f_1-f)}{sin\pi T_s(f_1-f)}\,cos2(\pi(N-1)T_s f_1+\psi)\right]^{\frac{1}{2}}. \qquad (3.9)$$

Fig. 3.1(b) illustrates this equation.

Comparing the FT of the truncated sequence to that of the infinite length sequence, the transform of the truncated signal is symmetrical about dc and integer multiples of the sampling frequency. The spectrum no longer consists of impulses, but has components at almost all frequencies. The introduction of the new frequency components is called smearing.[21]

Eqn. (3.9) is a special case of eqn. (3.8), because the sampling rate is synchronized to the frequency of the sampled signal. Therefore the truncation interval is equal to an integer number of periods, depending upon the value of N. This situation is possible if the frequency of the signal were already known. In this case computation of the FT of a signal would be redundant since the frequency spectrum is obvious. This very rarely occurs. Signals are often sampled asynchronously, because the frequency content is usually unknown. Hence the truncation interval is usually not equal to one period or any integer multiple of periods of the signal of interest.

As an example of what can happen to the spectrum of a truncated sequence, the dc component is considered. Eqn. (3.8) evaluated only at dc simplifies to:

$$X_T(1) = \frac{\sin(\pi f_1 T_s N)}{\sin(\pi f_1 T_s)} \cos(\pi f_1 T_s (N-1)+\psi). \qquad (3.10)$$

If the sampling rate is synchronized to f_1, then eqn. (3.10) reduces to zero, as shown in Fig. 3.1(b), where the magnitude of the FT goes to zero at dc. But if f_1 is not synchronized, then eqn. (3.10) does not reduce to zero. Therefore, with synchronous sampling, the truncation interval is equal to an integer multiple of the signal period and the value of the dc component of the FT is zero. When a signal is sampled asynchronously, the truncation interval is not equal to an integer multiple of the signal period and the truncated signal has a dc level introduced into its FT. The value of this dc level is determined by N, T_s, f_1 and ψ. However, ψ changes every time the data block takes in a new sample. Therefore, with N, T_s and f_1 constant, the dc component varies sinusoidally because the cosine term in eqn. (3.10) depends upon ψ.

3.3 WEIGHTING OF DISCRETE TIME SEQUENCES

The effect of truncation interval not equal to an integer number of periods is discussed in the previous section. The effect which results is known as smearing and is a common occurrence in digital signal processing. Since it is the frequency content of the signal that is usually under investigation, weighting techniques have been developed to minimize unwanted frequency components resulting from smearing.[22]

Weighting a data block before processing involves multiplying each data point $x_T(kT_s)$ by a weight $w(kT_s)$. Eqn. (3.6), which is the FT of the discrete time sequence $x_T(kT_s)$, is a weighting process. The weights are the real and imaginary components of the complex exponential

$e^{-j2\pi fkT_s}$ as shown below,

$$X_T(e^{j2\pi f}) = \sum_{k=-\infty}^{\infty} x_T(kT_s)\ [w(kT) + j\hat{w}(kT)] \tag{3.11}$$

where $$w(kT_s) = Re[e^{-j2\pi fkT_s}] = cos(2\pi fkT_s) \tag{3.12}$$

and $$\hat{w}(kT_s) = Im[e^{-j2\pi fkT_s}] = -sin(2\pi fkT_s). \tag{3.13}$$

The ^ over the w in eqn. (3.13) denotes that these weights are orthogonal to the weights defined by eqn. (3.12). Calculating $X_T(e^{j2\pi f})$ for all values of f will determine the frequency content of $x_T(kT_s)$ for the complete frequency spectrum.

Eqn. (3.10) defines the dc component of the FT of eqn. (3.2). The coefficient of the cosine term in this equation depends upon N, T_s and f_1. If N and T_s can be specified, then the coefficient is a function of f_1 only. The square of the magnitude of the coefficient of the cosine term in eqn. (3.10) is given by eqn. (3.14):

$$coeff[X_T(1)]^2 = \frac{sin^2(\pi f_1 T_s N)}{sin^2(\pi f_1 T_s)}\ . \tag{3.14}$$

Eqn. (3.14) is illustrated in Fig. 3.2. This figure shows that when N and T_s are specified, the magnitude squared results in a unique value for each value of f_1 from dc to the sample rate times N. In this range eqn. (3.14) is a measure of f_1, but this expression is derived from eqn. (3.10). Eqn. (3.10) by itself is of no use because the phase term, ψ, will change with each block of sampled data.

A weighting technique is required that can eliminate the phase dependent term and preserve the coefficient. Such a technique must take

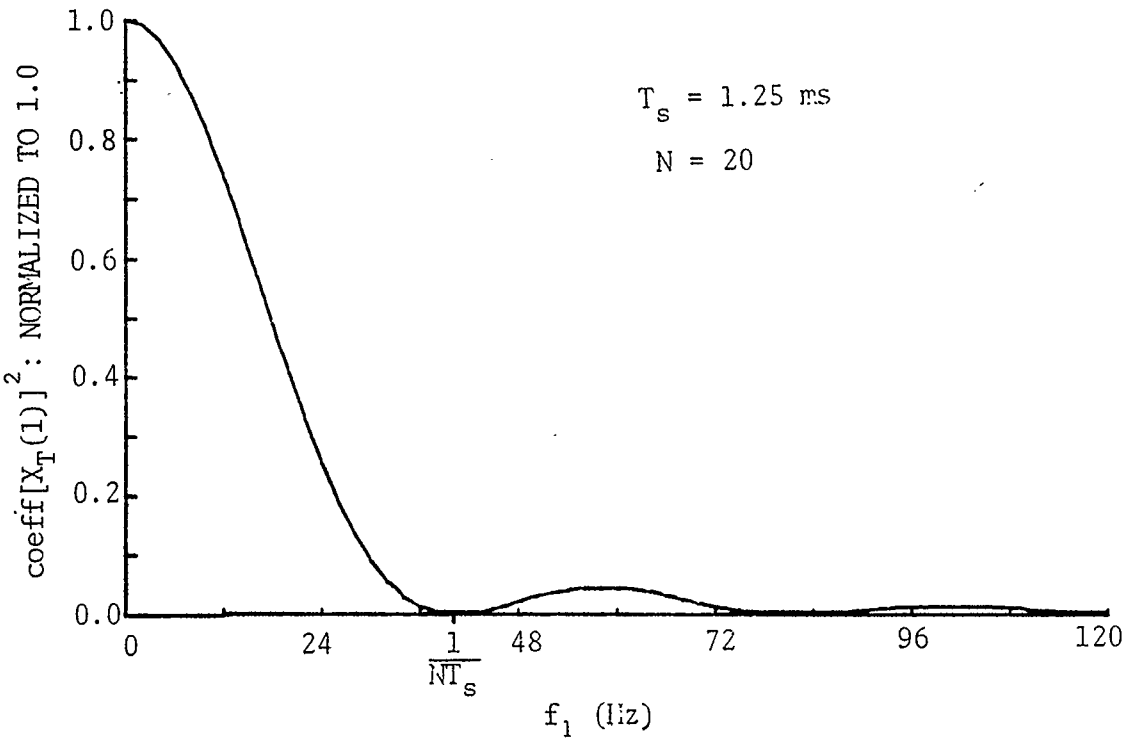

Fig. 3.2 Plot of coeff$[X_T(1)]^2$.

advantage of the smearing that occurs and, therefore, known techniques of weighting are of no use. Eqn. (3.11), when interpreted correctly, offers a possible method of solution. Therefore, it is by applying the FT of a discrete time sequence that a technique to estimate frequency will be derived. The proposed technique is described in the next section.

3.4 FREQUENCY MEASUREMENT USING A MODIFIED FOURIER TRANSFORM

3.4.1 A Modified Fourier Transform

The FT of a finite length discrete time sequence has been derived. Eqn. (3.10) is the result of this transform, when evaluated

at dc, and eqn. (3.14) is the square of the magnitude of the coefficient of the cosine term of this equation. Eqn. (3.14) is important because the value of this coefficient is a measure of the frequency of the sampled signal.

Unfortunately, the transform is dependent upon the phase of the sampled signal to that of the data block used by the transform. This phase dependence must be eliminated because the phase is unknown.

The proposed technique follows a procedure similar to the one used in section 3.2, except two signals are required and four summations are determined. These equations are manipulated to eliminate the phase dependent term. This time the result is not necessarily evaluated at dc but, as shown in Chapter 4, a reference frequency is chosen at which the estimate is most sensitive to f_1.

3.4.2 Evaluation of the Modified Fourier Transform

The modified form of the FT is found by simply evaluating eqn. (3.11) as two separate summations and not one. These summations are:

$$X_{1,T}(e^{j2\pi f}) = \mathrm{Re}[X_T(e^{j2\pi f})] = \sum_{k=-\infty}^{\infty} x_T(kT_s)\, cos(2\pi fkT_s) \qquad (3.15)$$

and

$$X_{2,T}(e^{j2\pi f}) = \mathrm{Im}[X_T(e^{j2\pi f})] = -\sum_{k=-\infty}^{\infty} x_T(kT_s)\, sin(2\pi fkT_s). \qquad (3.16)$$

If $x_T(kT_s)$ is replaced by eqn. (3.5), then the closed form of eqns. (3.15) and (3.16) are given by,

$$X_{1,T}(e^{j2\pi f}) = \frac{1}{2}\frac{sin\pi NT_s(f_1-f)}{sin\pi T_s(f_1-f)}\, cos(\pi(N-1)(f_1-f)T_s+\psi) + \frac{1}{2}\frac{sin\pi NT_s(f_1+f)}{sin\pi T_s(f_1+f)}$$

$$\times\, cos(\pi(N-1)(f_1+f)T_s+\psi) \qquad (3.17)$$

$$X_{2,T}(e^{j2\pi f}) = \frac{1}{2}\frac{sin\pi NT_s(f_1-f)}{sin\pi T_s(f_1-f)}\, sin(\pi(N-1)(f_1-f)T_s+\psi) - \frac{1}{2}\frac{sin\pi NT_s(f_1+f)}{sin\pi T_s(f_1+f)}$$

$$\times\, sin(\pi(N-1)(f_1+f)T_s+\psi). \qquad (3.18)$$

The method used to evaluate the closed form is similar to that used to evaluate the closed form for the FT of eqn. (3.2). This is given in Appendix I. If a signal that is orthogonal with $x_T(kT_s)$ is transformed then the result may be derived from

$$X_{3,T}(e^{j2\pi f}) = \sum_{k=-\infty}^{\infty} \hat{x}_T(kT_s)\, cos(2\pi fkT_s) \qquad (3.19)$$

and

$$X_{4,T}(e^{j2\pi f}) = -\sum_{k=-\infty}^{\infty} \hat{x}_T(kT_s)\, sin(2\pi fkT_s) \qquad (3.20)$$

where

$$\hat{x}_T(kT_s) = -sin(2\pi f_1 kT_s+\psi), \quad 0 \le k < N. \qquad (3.21)$$

Evaluating the closed form of eqns. (3.19) and (3.20) yields,

$$X_{3,T}(e^{j2\pi f}) = \frac{1}{2}\frac{sin\pi NT_s(f_1-f)}{sin\pi T_s(f_1-f)}\, sin(\pi(N-1)(f_1-f)T_s+\psi) + \frac{1}{2}\frac{sin\pi NT_s(f_1+f)}{sin\pi T_s(f_1+f)}$$

$$\times\, sin(\pi(N-1)(f_1+f)T_s+\psi) \qquad (3.22)$$

and

$$X_{4,T}(e^{j2\pi f}) = -\frac{1}{2}\frac{sin\pi NT_s(f_1-f)}{sin\pi T_s(f_1-f)}\, cos(\pi(N-1)(f_1-f)T_s+\psi) + \frac{1}{2}\frac{sin\pi NT_s(f_1+f)}{sin\pi T_s(f_1+f)}$$

$$\times\, cos(\pi(N-1)(f_1+f)T_s+\psi). \qquad (3.23)$$

Squaring eqns. (3.17) and (3.18) and summing the results yields,

$$X^2_{1,T}(e^{j2\pi f})+X^2_{2,T}(e^{j2\pi f}) = \frac{1}{4}\frac{sin^2\pi NT_s(f_1-f)}{sin^2\pi T_s(f_1-f)} + \frac{1}{4}\frac{sin^2\pi NT_s(f_1+f)}{sin^2\pi T_s(f_1+f)}$$

$$+ \frac{1}{2}\frac{sin\pi NT_s(f_1-f)sin\pi NT_s(f_1+f)}{sin\pi T_s(f_1-f)sin\pi T_s(f_1+f)}\, cos2(\pi(N-1)T_sf_1+\psi). \tag{3.24}$$

Applying the same procedure to eqns. (3.22) and (3.23) yields,

$$X^2_{3,T}(e^{j2\pi f})+X^2_{4,T}(e^{j2\pi f}) = \frac{1}{4}\frac{sin^2\pi NT_s(f_1-f)}{sin^2\pi T_s(f_1-f)} + \frac{1}{4}\frac{sin^2\pi NT_s(f_1+f)}{sin^2\pi T_s(f_1+f)}$$

$$- \frac{1}{2}\frac{sin\pi NT_s(f_1-f)sin\pi NT_s(f_1+f)}{sin\pi T_s(f_1-f)sin\pi T_s(f_1+f)}\, cos2(\pi(N-1)T_sf_1+\psi). \tag{3.25}$$

Adding eqns. (3.24) and (3.25) cancels any phase terms that are present and the result is,

$$X^2_{1,T}(e^{j2\pi f}) + X^2_{2,T}(e^{j2\pi f}) + X^2_{3,T}(e^{j2\pi f}) + X^2_{4,T}(e^{j2\pi f}) = \frac{1}{2}\left[\frac{sin^2\pi NT_s(f_1+f)}{sin^2\pi T_s(f_1+f)}\right.$$

$$\left. + \frac{sin^2\pi NT_s(f_1-f)}{sin^2\pi T_s(f_1-f)}\right]. \tag{3.26}$$

Eqn. (3.26) is dependent upon: the sampling rate, the number of samples that are weighted, the frequency at which this modified transform is evaluated and the frequency of the sampled signal. Since the first three terms are known a priori, eqn. (3.26) is a direct measure of the frequency of eqn. (3.2). The frequency at which this equation will be evaluated is discussed in the next chapter.

3.5 CONCLUSION

The effects of time domain truncation equal to one period and not equal to one period have been discussed. From this and the definition of the FT of a discrete time sequence a technique has been derived to estimate the frequency of a periodic signal. This technique is a hybrid form of the FT that weights samples of an orthogonal pair of signals to eliminate a phase term resulting from truncation not equal to an integer number of periods. The derived relationship is defined by eqn. (3.26). Specifying the sampling rate, the number of samples in the data block and the frequency at which this function is evaluated will result in eqn. (3.26) yielding a value directly proportional to the frequency of the sampled signal.

CHAPTER 4

IMPLEMENTATION OF THE PROPOSED TECHNIQUE

4.1 INTRODUCTION

A weighting procedure that can be used to estimate the frequency of a sinusoidal signal is discussed in Chapter 3. This technique can be implemented as an algorithm on a minicomputer to measure the angular speed of a rotating machine. The implementation described in this chapter is intended for application to the direct digital control of a turbine-generator unit.

Specifications for the digital measurement of speed in a stable electric power system are discussed in Chapter 1. Sensitivity, sampling rate and the data window size required to achieve these specifications are discussed and defined in this chapter.

4.2 THE TEST SIGNAL

The proposed digital frequency measurement technique estimates the frequency of a sinusoidal signal. Therefore, a transducer is needed to convert angular speed to electric frequency. If the speed of a turbine-generator is to be measured, then an ac tachogenerator (tach) coupled to the rotor will be a suitable transducer. The frequency of the ac signal generated from this tach is directly proportional to the mechanical speed of its rotor.[23] Thus, if the tach is coupled to the rotor of a turbine-generator unit, then the frequency of the voltage generated by the tach is directly proportional to the mechanical speed

of the turbine-generator.

The generated voltage of the tach is given by,[23]

$$x(t) = 2\pi f_1 K\Phi cos(2\pi f_1 t+\psi), \tag{4.1}$$

where f_1 is the frequency of $x(t)$, K is a constant dependent upon the number of conductors and how the armature is wound, and Φ is the air gap flux. If the coefficient of $cos(2\pi f_1 t+\psi)$ is held constant, this equation simplifies to

$$x(t) = A cos(2\pi f_1 t+\psi) \tag{4.2}$$

where

$$A = 2\pi f_1 K\Phi. \tag{4.3}$$

Eqn. (4.2) is in the form required for the derivation of eqn. (3.26). Therefore this signal can be used by the proposed technique to estimate the mechanical speed of a turbine-generator unit.

4.3 ORTHOGONAL SIGNAL PAIR

4.3.1 Direct and Quadrature Signals

The proposed technique of estimating the frequency is derived by assuming that a signal in quadrature with eqn. (4.2) is available. Letting eqn. (3.5) be the direct signal, the signal in quadrature is defined by eqn. (3.21). Together, these two signals form an orthogonal pair. Two methods of generating an orthogonal pair are:

(i) by generating it electrically with a two-phase tach,

(ii) or numerically, by calculating a signal in quadrature with the direct signal on a computer.

4.3.2 Generation of an Orthogonal Pair with a Two-Phase Tachogenerator

A two-phase tach is the most practical method of obtaining the orthogonal pair. A two-phase tach was not available for testing. So, as a compromise two single-phase tachs were used. One tach was coupled to the end of the rotor shaft and the second was coupled to the free end of the first tach. The connection between the tachs was designed so that the shaft of the second tach could be rotated relative to the first. By physically rotating the second tach, the signal generated from this tach could be displaced 90 degrees electrical with respect to the first tach. In this way the two single-phase tachs simulated a two-phase tach.

This arrangement has two disadvantages. Both tachs must have identical characteristics and the phase relationship between the direct and quadrature signals must be exactly 90 degrees for the signals to be orthogonal. If this relationship does not exist, then the estimate will oscillate about a dc value at twice the frequency of the signal being measured, because the phase-dependent terms in eqns. (3.24) and (3.25) will not cancel when these functions are added together.

A pair of tachs that could generate a signal at the same amplitude when rotating at the same speed could not be found. Also, with two tachs that had similar characteristics the phase between the generated voltages could not be resolved to better than 0.5 degrees. Due to these difficulties, the procedure adopted was to calculate the quadrature signal numerically.

4.3.3 Numerical Calculation of the Quadrature Signal

Calculation of the quadrature signal from sampled values of the direct signal is a two part process. The first part calculates the

magnitude of the quadrature signal and the second part determines the sign of this signal.

4.3.3.1 Calculation of the magnitude

If two signals x(t) and y(t) are sinusoidal, have an amplitude A, oscillate at the same frequency and satisfy

$$A^2x^2(t) + A^2y^2(t) = A^2, \tag{4.4}$$

then these two signals form the required orthogonal pair. This equation may be normalized by dividing both sides by A^2. The result is

$$x^2(t) + y^2(t) = 1. \tag{4.5}$$

Since y(t) is orthogonal to x(t), it can be replaced by $\hat{x}(t)$. Solving eqn. (4.5) for $\hat{x}(t)$ results in eqn. (4.6):

$$|\hat{x}(t)| = \sqrt{1-x^2(t)}\ . \tag{4.6}$$

Therefore, by normalizing x(t) the magnitude of the signal in quadrature with x(t) can be calculated by using eqn. (4.6).

4.3.3.2 Decision process for the sign of the orthogonal signal

A pair of signals that can be used by the frequency measurement algorithm are:

$$x(t) = cos(2\pi f_1 t+\psi) \tag{4.7}$$

and

$$\hat{x}(t) = -sin(2\pi f_1 t+\psi). \tag{4.8}$$

A result similar to eqn. (4.8) may be found by evaluating the first derivative of x(t) with respect to time as follows:

$$\frac{dx(t)}{dt} = -2\pi f_1 sin(2\pi f_1 t+\psi). \qquad (4.9)$$

Normalizing eqn. (4.9) yields the same result as eqn. (4.8). Hence, eqns. (4.7) and (4.8) are related by finding the derivative of x(t). An orthogonal signal for use in measuring f_1 cannot be evaluated using this technique because f_1 must be known to normalize eqn. (4.9). However, this equation is of some use.

Eqn. (4.9) shows that the sign of the derivative of the direct signal and that of the quadrature signal is the same. This is illustrated in Fig. 4.1 which illustrates two cycles of eqns. (4.7) and (4.8) when ψ equals 0. When x(t) is decreasing the sign of $\hat{x}(t)$ is negative, and when x(t) is increasing the sign of $\hat{x}(t)$ is positive. Therefore, the sign of the quadrature signal can be determined from the slope or first derivative of the direct signal.

This procedure will work with continuous signals, but when discrete signals are used a problem arises in determining the slope. Referring to Fig. 4.2, both points a´ and b´ are samples of x(t). The samples that preceded a´ and b´ are given by a and b respectively. The respective slopes at a´ and b´ are estimated by subtracting the preceding samples from the present samples. The first difference has a positive sign indicating that at point a´, x(t) is increasing. But as shown in Fig. 4.2, x(t) is decreasing at a´. Similarly, the second difference has a negative sign indicating that at point b´, x(t) is decreasing. Again Fig. 4.2 shows that at b´, x(t) is actually increasing.

This problem occurs only when x(t) is changing through either a positive or a negative maximum. The reason for this problem is the

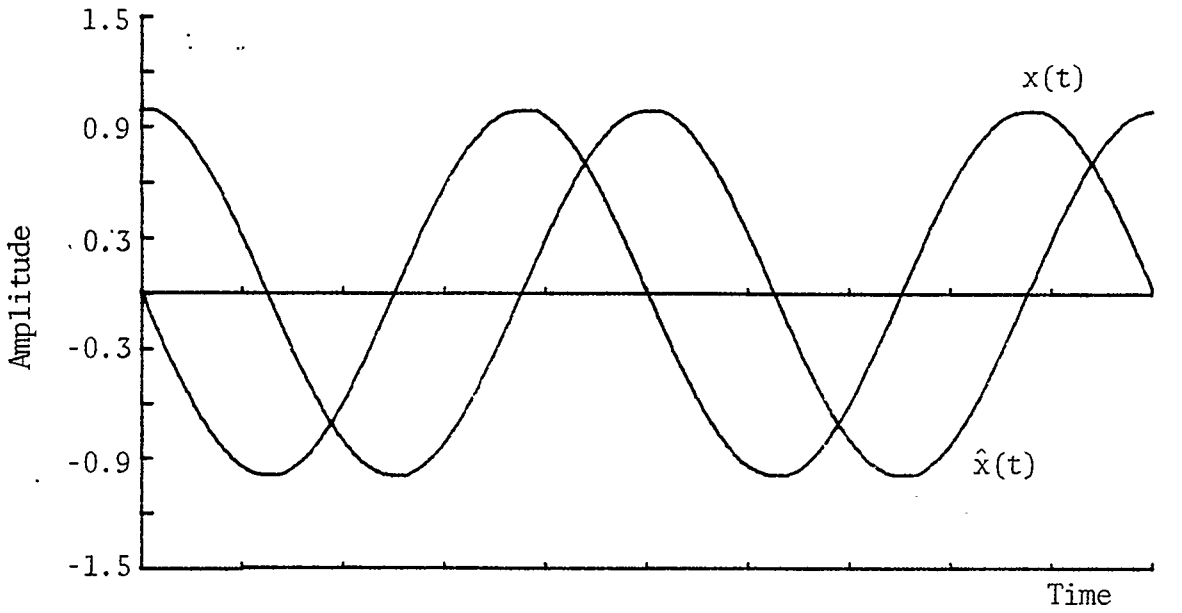

Fig. 4.1 Two cycles of $x(t)$ and $\hat{x}(t)$.

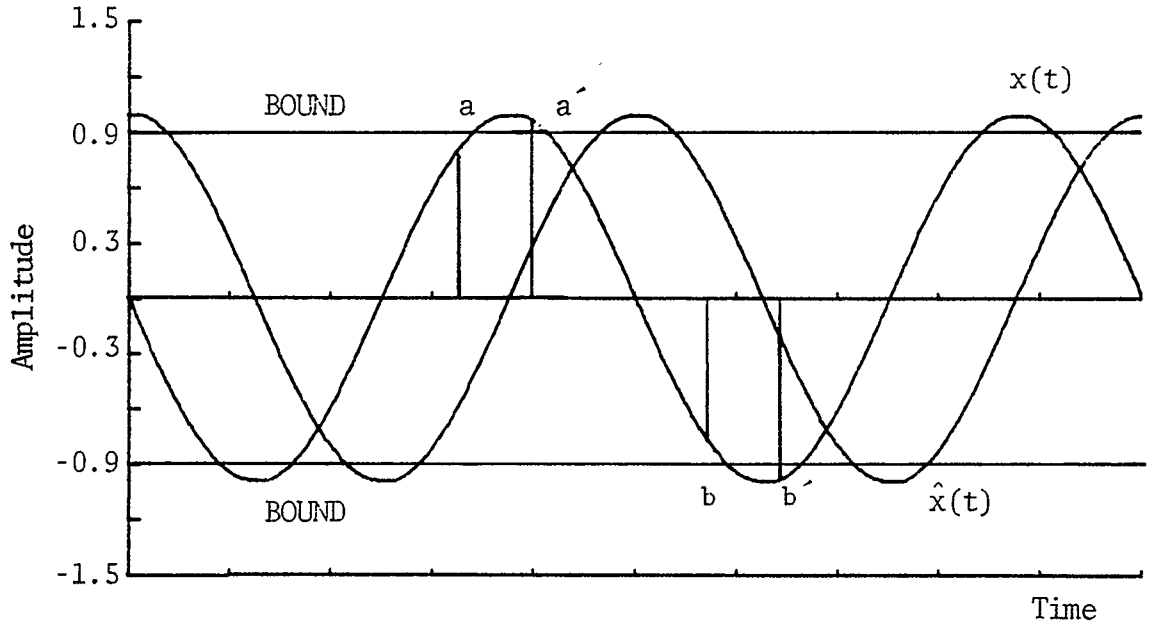

Fig. 4.2 Two cycles of an orthogonal pair showing sample points near the positive and negative maximums.

approximation involved by only having knowledge of the sample points. The derivative of x(t) changes sign at a positive or a negative maximum. With sampled data this is not apparent until at least two samples after the derivative changes sign.

The error introduced by calculating an orthogonal signal this way can be reduced by sampling faster. The error decreases because an increased sampling rate decreases the time required to sense a change in the direction of slope. A sampling rate sufficiently fast to introduce very little error, in generating the quadrature signal, would be too fast for the computer to process the data in real-time. Therefore, an alternate method is required.

From a knowledge of the variations in the frequency of the direct signal and of the sampling rate, a bound can be determined. This bound is shown in Fig. 4.2. The level of the bound is chosen such that if the value of a signal is above the positive bound or below the negative bound, then the slope of x(t) changed sign with this sample or will change sign during the next sampling interval.

This method requires that the present sample be stored so that it may be compared with the next sample. A flow chart outlining this procedure is shown in Fig. 4.3. At the start of the flow chart the next to last sample is compared with the bound. If it is within the positive and negative bounds, then the sign of $\hat{x}(kT_s)$ is determined from the difference of the last sample and the next to last sample. If the next to last sample is not within the positive and negative bounds, then the sign of $\hat{x}(kT_s)$ is the opposite of the sign of $x(kT_s)$.

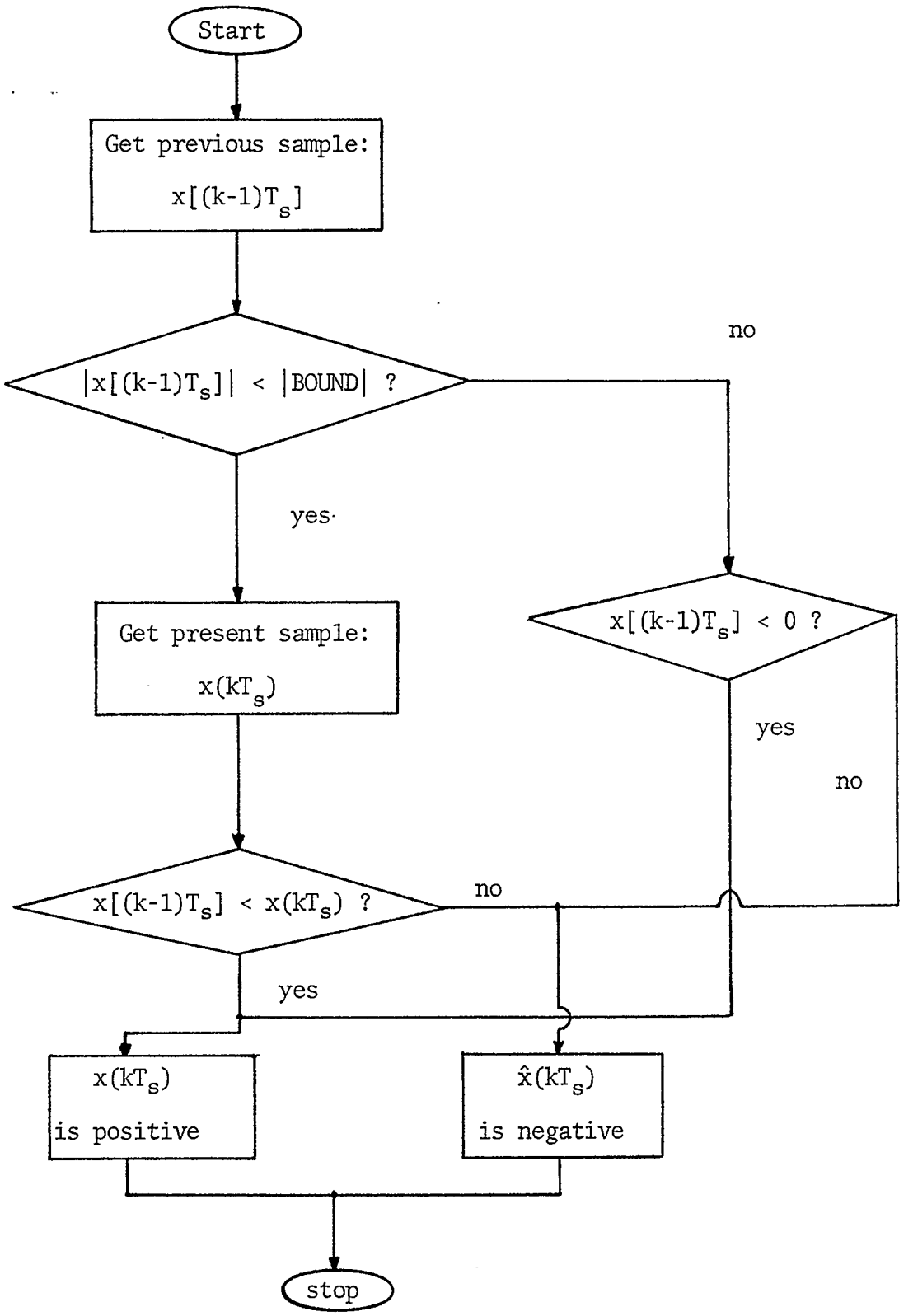

Fig. 4.3 Flow chart to determine the sign of the quadrature signal.

4.4 ALGORITHM USED TO ESTIMATE SPEED

An algorithm based upon the derivation of eqn. (3.26) has been written for application to the solution of the angular speed measurement problem. A flow chart of this algorithm is described in Fig. 4.4. The flow chart includes all aspects required to write a program which applies the frequency estimating technique proposed in Chapter 3.

This algorithm has two stages: initialization stage and continuation stage. The functions of these are described below.

4.4.1 Initialization Stage

Initialization is the first stage of the algorithm. It is outlined by dashes in Fig. 4.4. The procedure that must be followed in the initialization stage is to calculate the constants that are required for the algorithm and solve the following equations once, with ℓ equal to 1 to represent the first estimate:

$$X_1(\ell) = \sum_{k=1}^{N} x(kT_s)\, w(kT_s) \tag{4.10}$$

$$X_2(\ell) = \sum_{k=1}^{N} x(kT_s)\, \hat{w}(kT_s) \tag{4.11}$$

$$X_3(\ell) = \sum_{k=1}^{N} \hat{x}(kT_s)\, w(kT_s) \tag{4.12}$$

$$X_4(\ell) = \sum_{k=1}^{N} \hat{x}(kT_s)\, \hat{w}(kT_s) \tag{4.13}$$

and

$$E(\ell) = X_1^2(\ell) + X_2^2(\ell) + X_3^2(\ell) + X_4^2(\ell). \tag{4.14}$$

The first four of these equations are the ones used to derive eqn. (3.26). $x(kT_s)$ are sampled values of the signal of the ac tach,

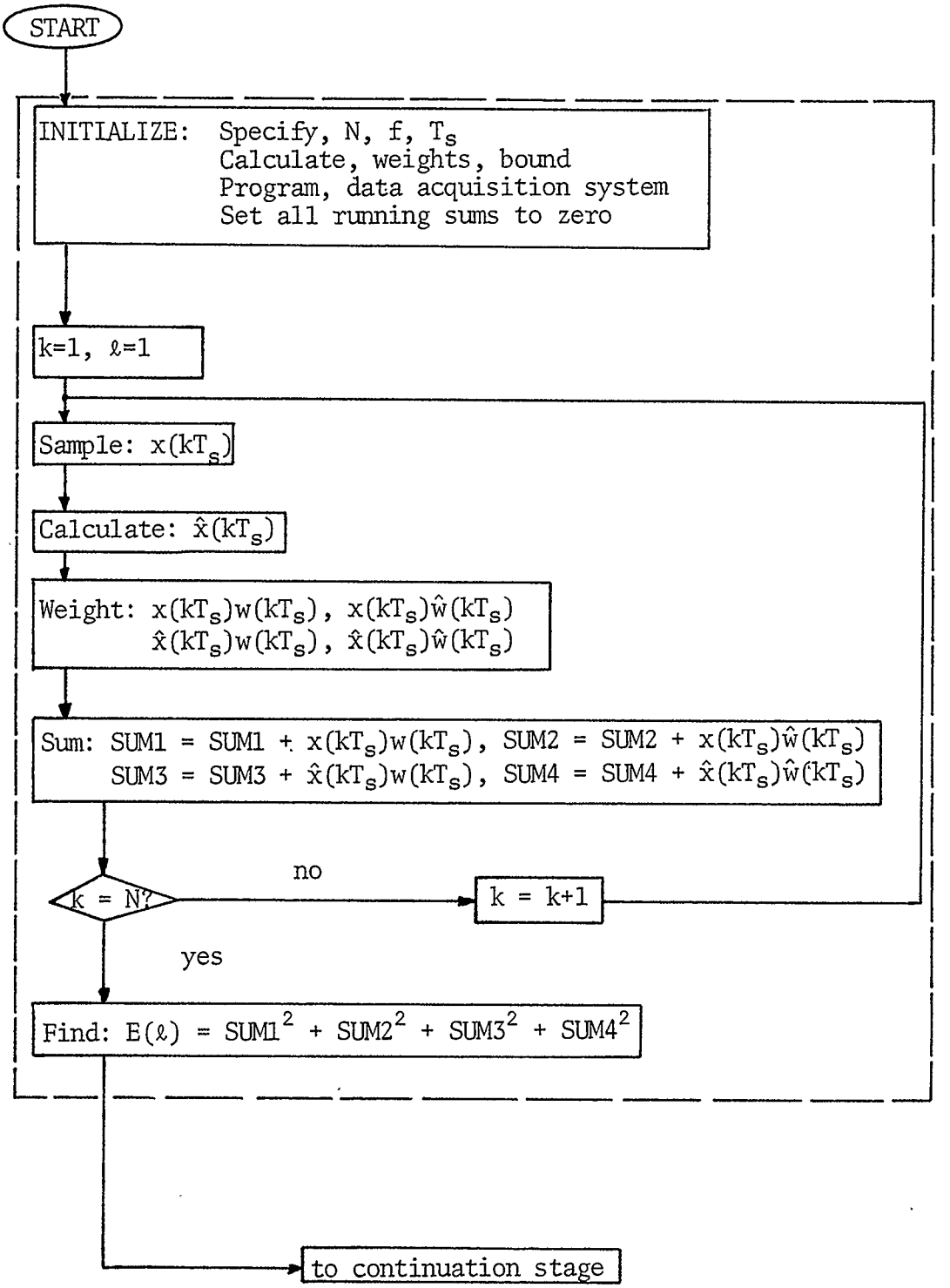

Proceed to continuation stage

Fig. 4.4(a) Initialization stage.

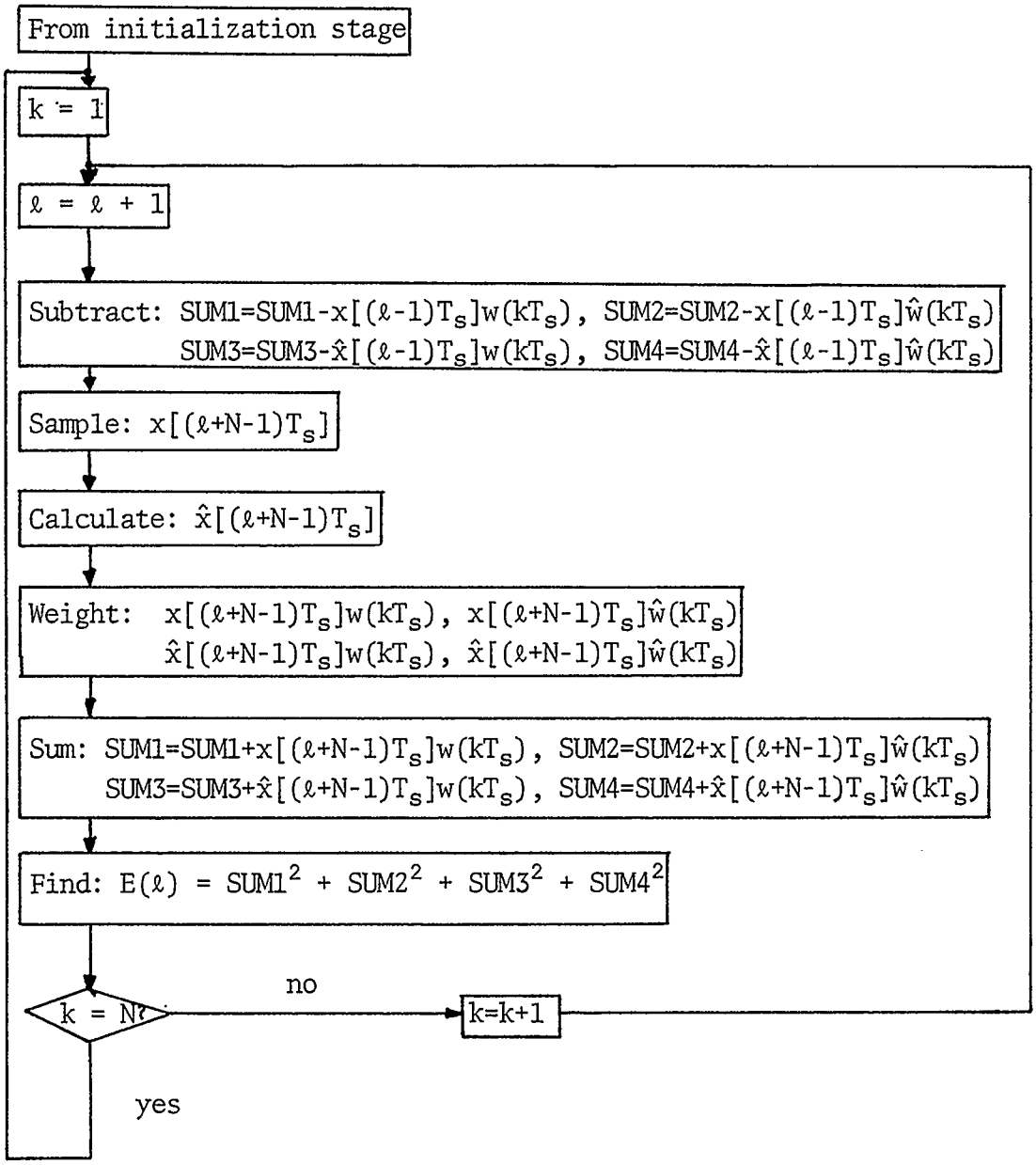

Fig. 4.4(b) Continuation stage.

and $\hat{x}(kT_s)$ are the calculated samples of the signal that is in quadrature with $x(t)$. $w(kT_s)$ and $\hat{w}(kT_s)$ are the weights that were used to derive eqn. (3.26). They are calculated by evaluating eqns. (3.12) and (3.13) with f equal to the frequency at which eqn. (3.26) is evaluated. A sinusoidal signal oscillating at f Hz is called the reference and the weights are called weights of the reference. The frequency of the reference is chosen by a procedure described in section 4.5. Eqn. (4.14) is identical to eqn. (3.26). It represents the speed estimate that is based on the N previous samples.

The block in Fig. 4.4 labeled "initialize" will determine the frequency of the reference and the number of weights required for the estimate. From these the weights are calculated, the sampling rate is determined, the bounds required for the calculation of $\hat{x}(kT_s)$ are calculated and the data acquisition system is programmed. Finally, a data sample is taken to initiate the routine that determines the sign of the quadrature data.

Another data sample is taken and the sample in quadrature with this is calculated. Then the first terms of eqns. (4.10) to (4.13) are determined by multiplying the direct and quadrature data both by the direct and quadrature weights. These products are added to the running sums which were equal to zero since this is the first sample. This procedure repeats until N samples are acquired.

After the first N samples have been acquired and processed, the first estimate is calculated by determining the sum of the square of the running sums as defined by eqn. (4.14). This estimate is directly proportional to the frequency of the sampled sinusoid. Once the first estimate has been made, the algorithm proceeds to the continuation

stage.

4.4.2 Continuation Stage

An estimate is made for each sampling instant in the continuation stage. This estimate is based only on the N most recent samples. Therefore, before each sample is taken the running sums are adjusted by subtracting the products that were calculated N samples preceding the present sampling instant.

A sample is acquired and the data value in quadrature with this is calculated. These are weighted and added to the running sums as before. An estimate is made and then the procedure repeats for all successive samples.

4.5 SPECIFICATION OF THE ALGORITHM

4.5.1 Choice of f, N and T_s

The theoretical value that is proportional to the frequency of the ac signal from the tach is defined by eqn. (3.26). This equation is rewritten below:

$$E(N,T_s,f_1,f) = \frac{1}{2}\left[\frac{sin^2\pi NT_s(f_1+f)}{sin^2\pi T_s(f_1+f)} + \frac{sin^2\pi NT_s(f_1-f)}{sin^2\pi T_s(f_1-f)}\right]. \qquad (4.15)$$

With N, T_s and f specified, f_1 can be measured by applying the algorithm described in the previous section. Selection of the best combination of N, T_s and f is decided by solving eqn. (4.15) for certain values of N, a range of values of f and an assumed value of f_1. The assumed value of f_1 is 60 Hz for this application, since the range of interest is the fluctuations about 60 Hz that are present when the tach is coupled to a turbine-generator set running at rated speed.

The weights are calculated from a sinusoid of the same frequency as the reference. The sampling rate is related to f by N because the block of weights used to estimate f_1 has a finite length of N. This relationship is

$$T_s = \frac{1}{Nf} . \tag{4.16}$$

So by selecting f and N, T_s is determined automatically; or by selecting T_s and N, f can be determined. Thus only two of the three parameters, N, T_s and f, need be specified.

There is a constraint on the value of T_s. For real-time applications, the time required to execute the continuation section of the speed measurement algorithm must be less than T_s. This execution time depends on the type of device used and upon how the algorithm is written for application on this device. The execution time for the continuation stage is 1.25 ms when this algorithm is written in assembly language and run on an HP 21MXE minicomputer.

Fig. 4.5 illustrates the solution of eqn. (4.15) for three values of N, f_1 equal to 60 Hz and f varying from 20 to 120 Hz. The magnitude of E changes most rapidly between 30 and 50 Hz. The maximum value of E occurs at 60 Hz and is given by,

$$\text{Max}[E] \cong \frac{N^2}{2} . \tag{4.17}$$

It can be seen from Fig. 4.5 that the best value of f is between 30 and 50 Hz, because the estimate changes rapidly in this region. To find the exact value of f, the partial derivative of eqn. (4.15) with respect to f is obtained giving,

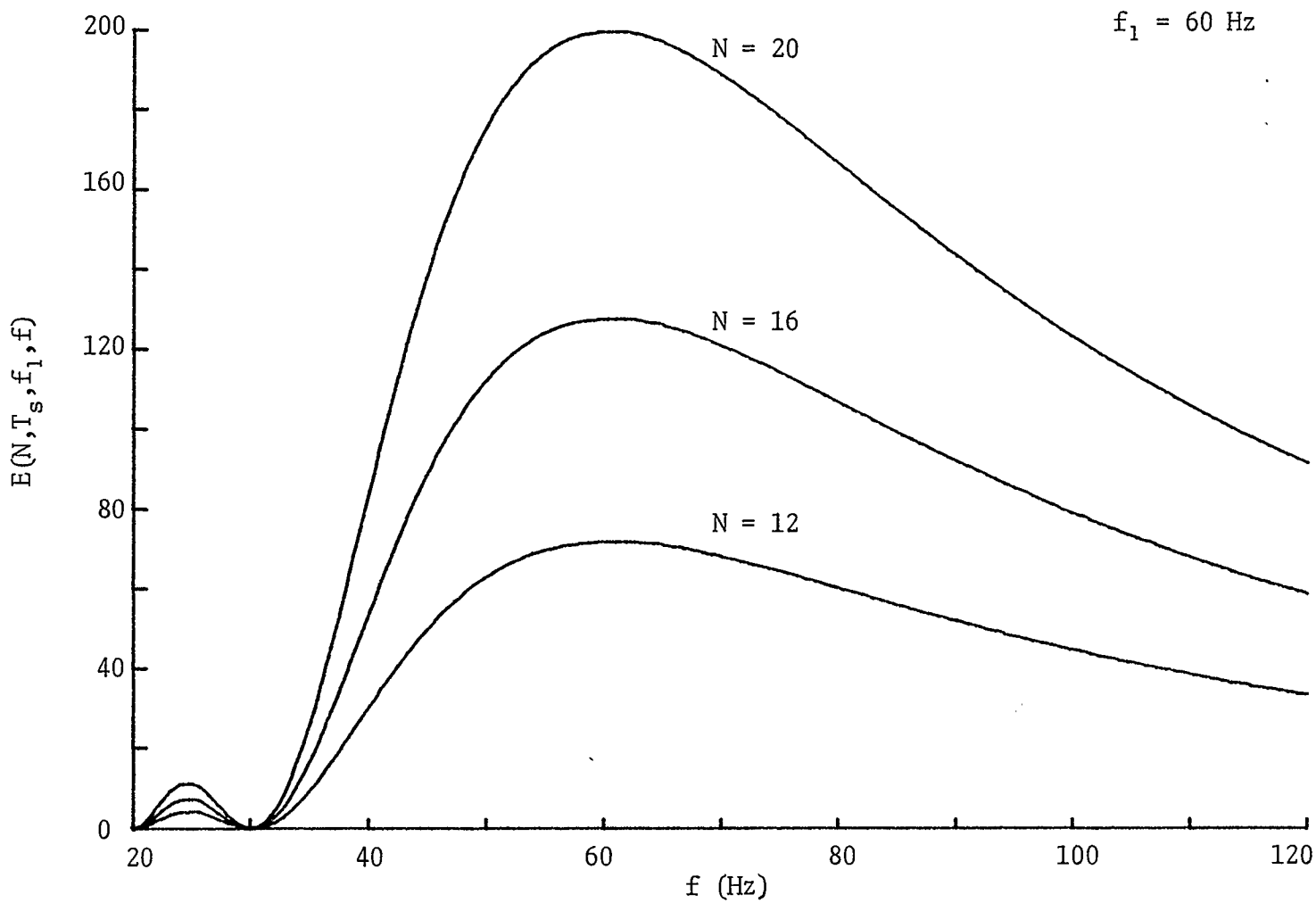

Fig. 4.5 Solutions of eqn. (4.15): Varying reference frequency.

$$\frac{\partial E}{\partial f}(N,T_s,f_1,f) = \pi \frac{sin\pi NT_s(f_1-f)}{sin^3\pi T_s(f_1-f)} \cdot \frac{(-f^2+f-f_1)}{f^2} [sin\pi T_s(f_1-f)\ cos\pi NT_s(f_1-f) - \frac{1}{N} sin\pi NT_s(f_1-f)\ cos\pi T_s(f_1-f)]$$

$$+ \pi \frac{sin\pi NT_s(f_1+f)}{sin^3\pi T_s(f_1+f)} \cdot \frac{(f^2-f-f_1)}{f^2} [sin\pi T_s(f_1+f)\ cos\pi NT_s(f_1+f) - \frac{1}{N} sin\pi NT_s(f_1+f)\ cos\pi T_s(f_1+f)]. \quad (4.18)$$

The maximum value of this equation is the maximum slope of eqn. (4.15). The reference frequency where the maximum occurs is the ideal value of the reference that is used to calculate the weights in the initialization stage algorithm. Solutions of eqn. (4.18), for the same values of N as in Fig. 4.5, are shown in Fig. 4.6.

Numerical solution of eqn. (4.18) indicates that the best reference frequency is 39 Hz. This is shown by the maximums that occur for each plot in Fig. 4.6. The maximum slope for the three plots occurs when N is largest; N equal to 20 in this case.

Fig. 4.7 illustrates the solution of eqn. (4.15), for the same values of N as in Figs. 4.5 and 4.6, solved by varying f_1 from 20 to 120 Hz with f equal to 39 Hz. This figure verifies that E is most sensitive to fluctuations in f_1 about 60 Hz when f is equal to 39 Hz.

So if f was chosen to be 39 Hz and N was chosen to be 20, then the sampling rate is 1.28 ms. The execution time between samples is 1.25 ms so data can still be acquired in real-time. The estimate is updated once every 1.28 ms because an estimate is made for every sample taken. This estimate is based upon the 20 most recent samples or one period of the reference, which for this case is 26 ms.

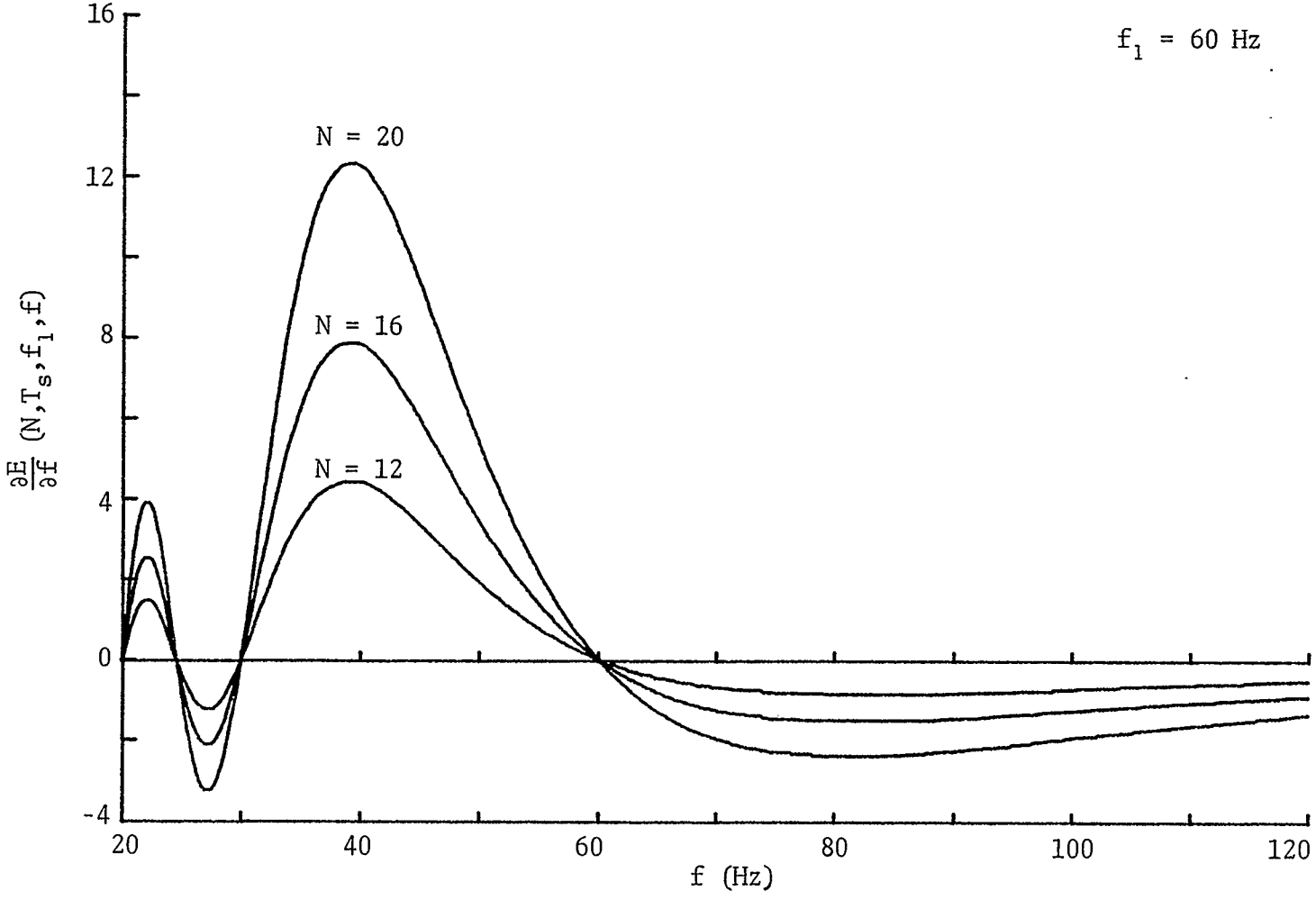

Fig. 4.6 Solutions of eqn. (4.18):
Partial derivative of eqn. (4.15) with respect to the reference frequency.

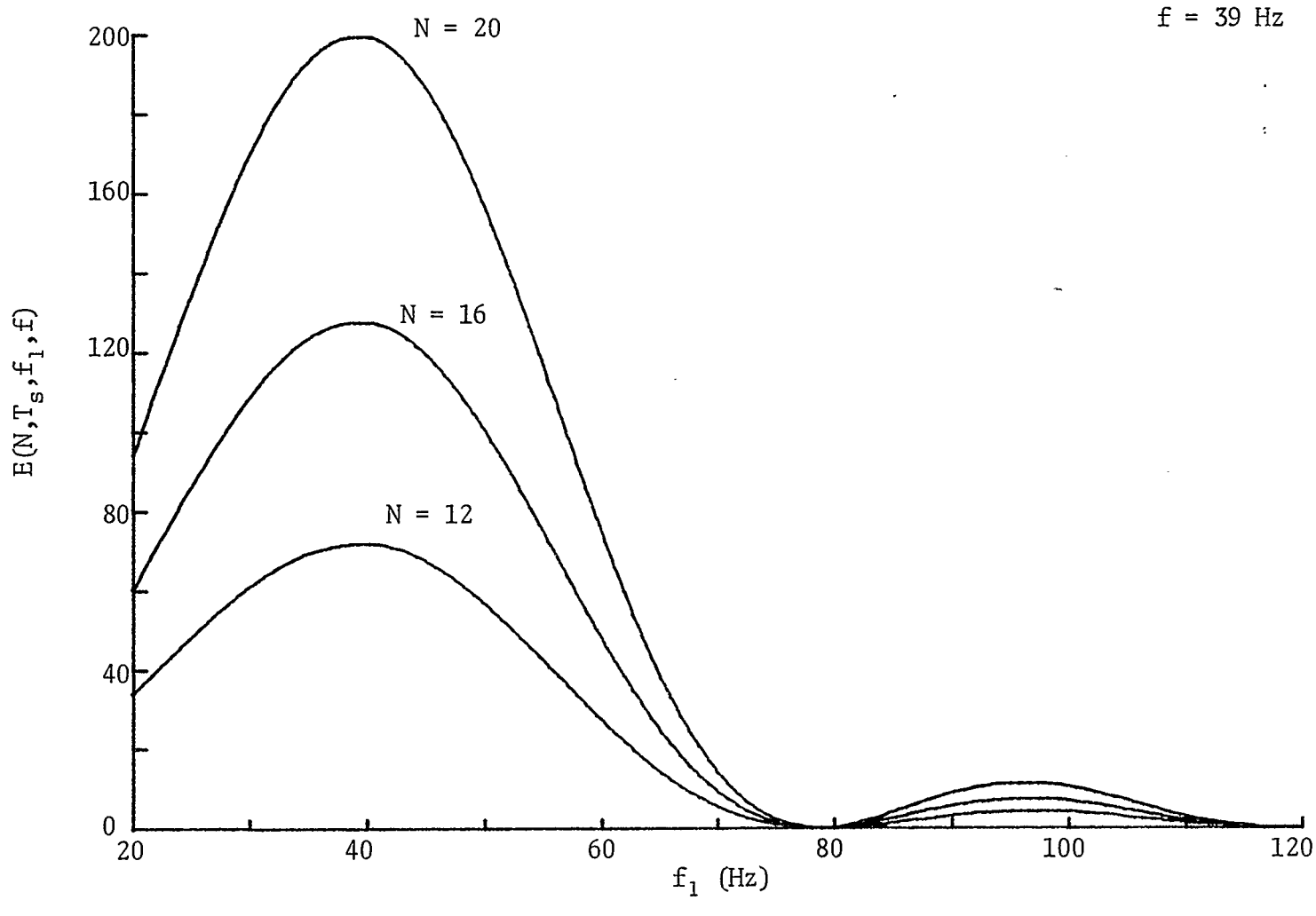

Fig. 4.7 Solutions of eqn. (4.15): Varying unknown frequency.

4.5.2 Sensitivity

Fig. 4.7 illustrates the solution of eqn. (4.15). The horizontal axis is the frequency of the signal generated by the tach, and the vertical axis is the theoretical estimate calculated for each value of f_1. It can be seen that the correspondence between estimate and frequency is not unique. However, if the range of values for f_1 is constrained to a narrow portion of the horizontal axis, then it is possible to define a unique value of the estimate for each frequency within the constrained range.

A common characteristic of steam turbine-generators is that they are operated within a range that is ±4% of rated speed.[24,25] Fig. 4.8 illustrates the solution of eqn. (4.15) with N equal to the same values as in Fig. 4.7, f equal to 39 Hz and f_1 constrained to 60 ± 2.4 Hz. This range of values for f_1 corresponds to a ±4% change in the rated speed of a turbine-generator. It can be seen that on this graph each estimate corresponds to only one frequency.

The curve for N equal to 20 defines where the algorithm is most sensitive to the frequency. A 4% change in frequency results in a 25% change in the estimate.

Fig. 4.9 illustrates 100 consecutive estimates made on data that was simulated with a computer. The estimates were calculated with N=20 and f=39 Hz. Also the estimates were normalized so that 1 is equal to 60 Hz or rated speed. Each line on Fig. 4.9 corresponds to a different value of f_1. These estimates are made after the initialization.

Table I is a list of the normalized values of the estimate of frequencies close to 60 Hz. These estimates do not yield distinct lines when illustrated on plots like Fig. 4.9. However, Table I shows that a

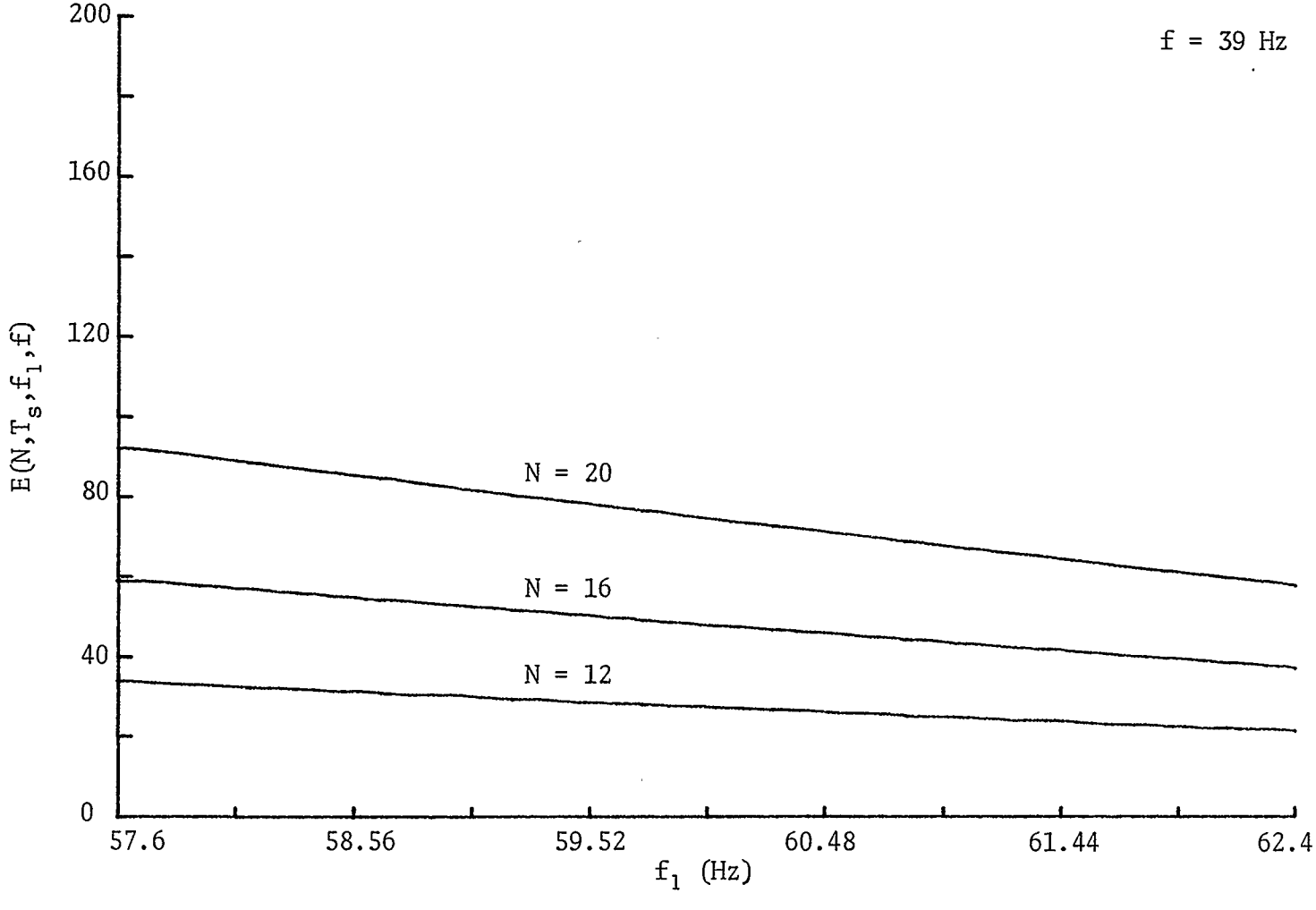

Fig. 4.8 Solutions of eqn. (4.15): Varying unknown frequency.

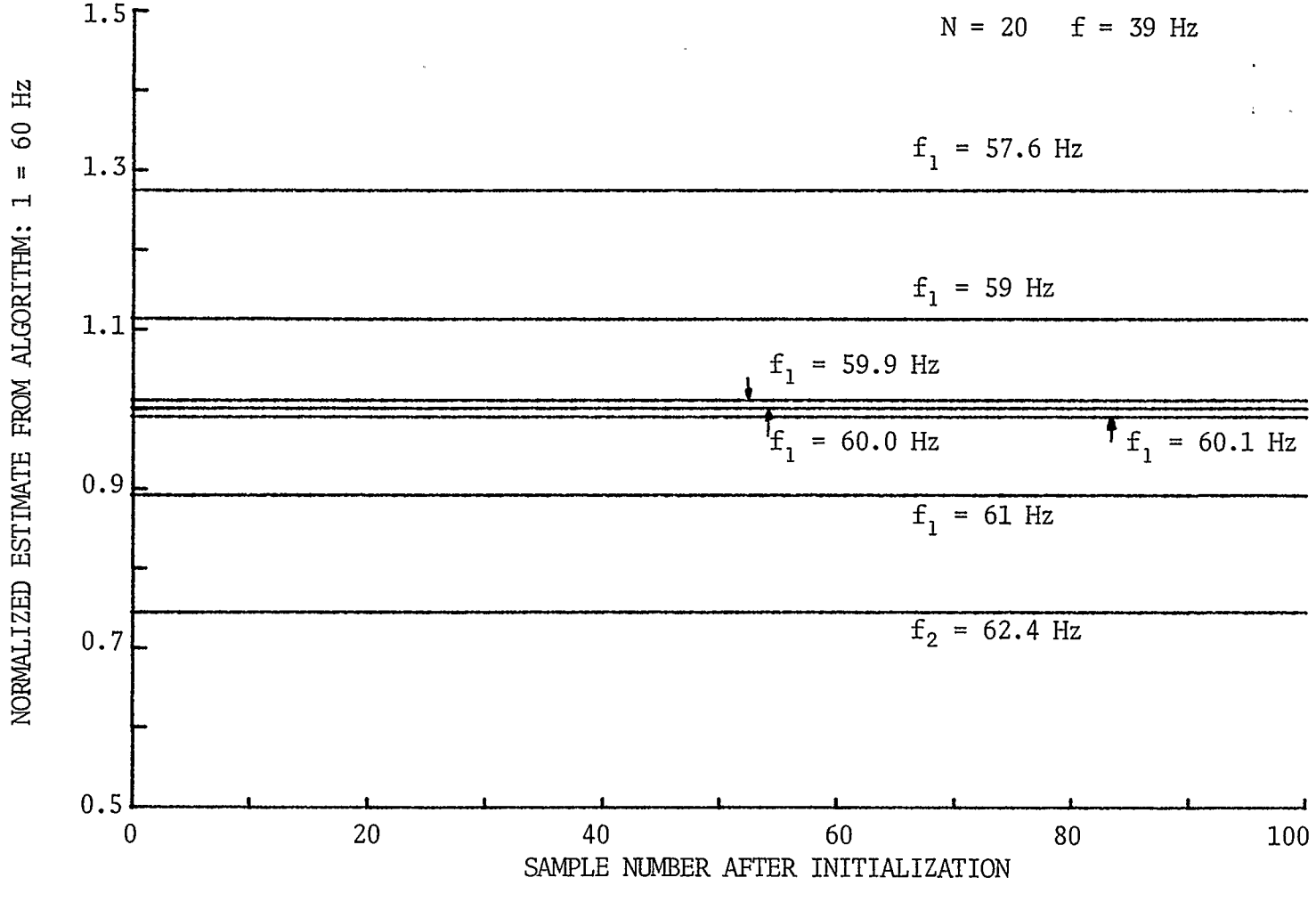

Fig. 4.9 Estimates of frequency based on simulated data samples.

resolution of 0.01 Hz is possible because the estimates made are for frequencies that are 0.01 Hz apart.

TABLE I

NORMALIZED ESTIMATE OF FREQUENCY

f = 39 Hz N = 20

FREQUENCY	ESTIMATE	FREQUENCY	ESTIMATE
59.90	1.011133	60.00	1.000000
59.91	1.010018	60.01	0.998888
59.92	1.008904	60.02	0.997778
59.93	1.007789	60.03	0.996668
59.94	1.006675	60.04	0.995558
59.95	1.005561	60.05	0.994447
59.96	1.004449	60.06	0.993338
59.97	1.003336	60.07	0.992229
59.98	1.002223	60.08	0.991121
59.99	1.001112	60.09	0.990013
		60.10	0.988905

4.5.3 Resolution of A/D Conversion

This technique calculates the estimate of the frequency of a sinusoid with knowledge of the amplitude versus time information acquired from waveform sampling. Fig. 4.8 illustrates that the frequency resolution is linearly dependent on the resolution of the estimate. However, the resolution of the estimate depends upon that of the amplitude of the sampled signal.

If eqn. (3.26) is derived by including a term to represent amplitude in eqns. (3.5) and (3.21), then the result would have been,

$$E(N,T_s,f_1,f) = \frac{A^2}{2}\left[\frac{sin^2\pi NT_s(f_1+f)}{sin^2\pi T_s(f_1+f)} + \frac{sin^2\pi NT_s(f_1-f)}{sin^2\pi T_s(f_1-f)}\right] \qquad (4.19)$$

where the amplitude term is represented with the letter "A". Eqn. (4.19) shows that the estimate of f_1 is proportional to the square of the amplitude of the sampled signal. Therefore, the resolution of the estimate is related to the resolution of the amplitude.

By specifying the required resolution of f_1, the resolution of E is defined, which defines the resolution of A. Knowing this, the size of the A/D converter in the data acquisition system can be specified, because the resolution of A is determined by the resolution of the A/D converter.

The required resolution of E may be represented by B and the error from A/D conversion can be represented by ε. The maximum error allowed will define the resolution of the A/D converter so that if this error exists the absolute difference between the ideal estimate defined by eqn. (4.18) and the estimate that includes the error is less than the desired resolution of E. Eqn. (4.20) describes this mathematically, i.e.,

$$|E(N,T_s,f_1,f) - E_\varepsilon(N,T_s,f_1,f)| \leq BE(N,T_s,f_1,f). \qquad (4.20)$$

The subscript ε in this equation indicates that this estimate includes an error from the A/D conversion. The error is included by replacing A with $A+\varepsilon$ in eqn. (4.19). Dividing the common terms out of eqn. (4.20) yields,

$$2A\varepsilon + \varepsilon^2 \leq BA^2. \qquad (4.21)$$

If ε is small, then ε^2 will have a negligible effect on this equation so it is dropped out. Solving eqn. (4.21) yields

$$\varepsilon \leq \frac{BA}{2}. \qquad (4.22)$$

Thus, if the required resolution of the estimate is 0.1% and if A is 10 volts, then ε is in volts and is given by

$$\varepsilon \leq 0.005. \tag{4.23}$$

As assumed above, ε is a small value. The resolution of the A/D converter required to ensure that ε satisfies eqn. (4.23) is 11 bits or more, given that the range of the converter is ±10 volts.

4.6 CONCLUSION

The weighting technique discussed in Chapter 3 can be applied to measure the angular speed of a turbine-generator unit. This is done by measuring the frequency of the ac voltage from a permanent magnet tach rigidly coupled to the turbine-generator rotor shaft. This technique is implemented digitally on a minicomputer. The sensitivity of the technique depends upon the sampling rate used. This sampling rate is limited by the execution time of the algorithm. It has been shown that the proposed technique is most sensitive when the estimate is evaluated using a reference waveform at a frequency of 39 Hz. Chapter 5 discusses static and transient tests on the proposed technique and on the constant displacement shaft-encoder.

CHAPTER 5

STATIC AND DYNAMIC TESTS

5.1 INTRODUCTION

Practical tests were performed on the constant-displacement shaft-encoder and the proposed technique of digital angular speed measurement which relies on waveform sampling to produce an estimate of angular velocity. The tests performed are used to evaluate and compare both methods of speed measurement.

Two different tests were performed: (i) a static test, which is a test performed on a constant frequency speed signal, and (ii) a dynamic test, which is one performed on a speed signal that changes from one speed to another. Static tests are used to evaluate the resolution of a measurement technique and dynamic tests are used to evaluate the ability of a technique to follow a change in speed.

5.2 PHYSICAL APPLICATION OF BOTH TECHNIQUES

5.2.1 Constant-Displacement Shaft-Encoder

Tests applying this technique were performed using a laboratory setup similar to the one described in Fig. 2.1. In this case a dc machine was used as the prime mover.

A block diagram of the circuit designed to apply this technique is illustrated in Fig. 5.1(a). All the components of this circuit were constructed with standard TTL building blocks, except for the opto-coupler which in this case is a photo-diode.

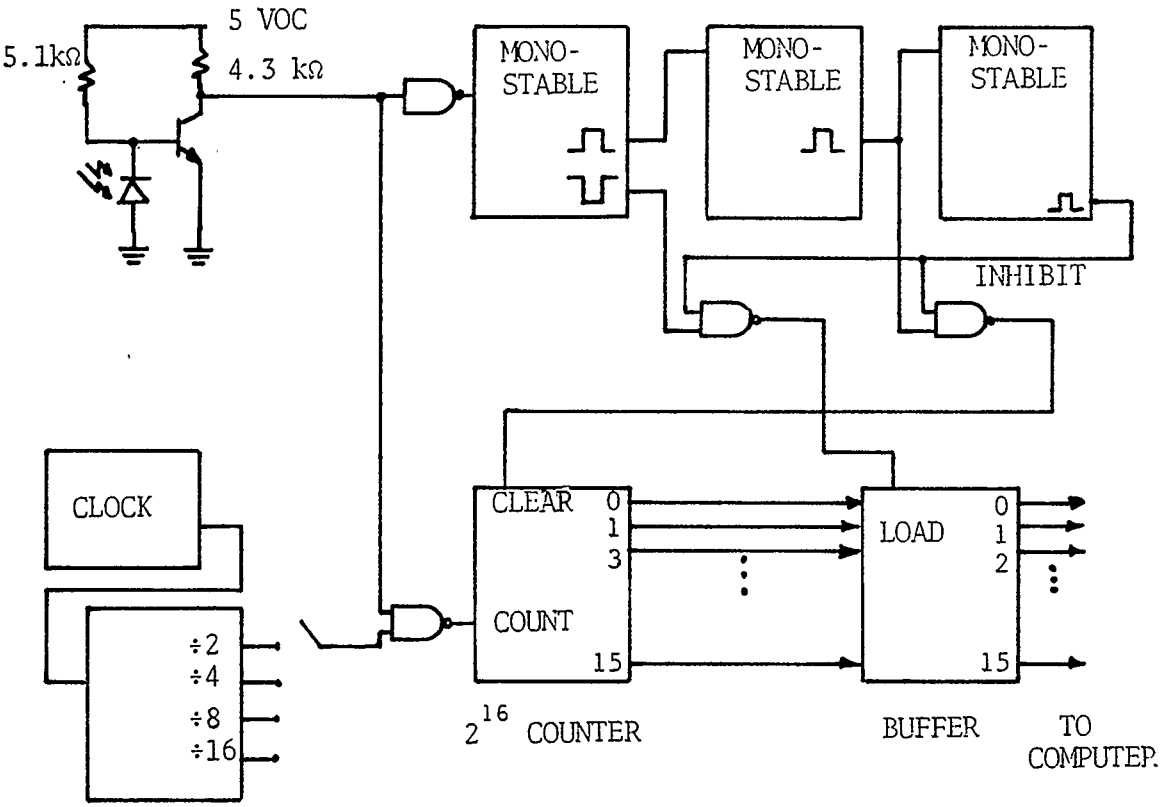

Fig. 5.1(a) Block diagram of shaft-encoder measurement circuit.

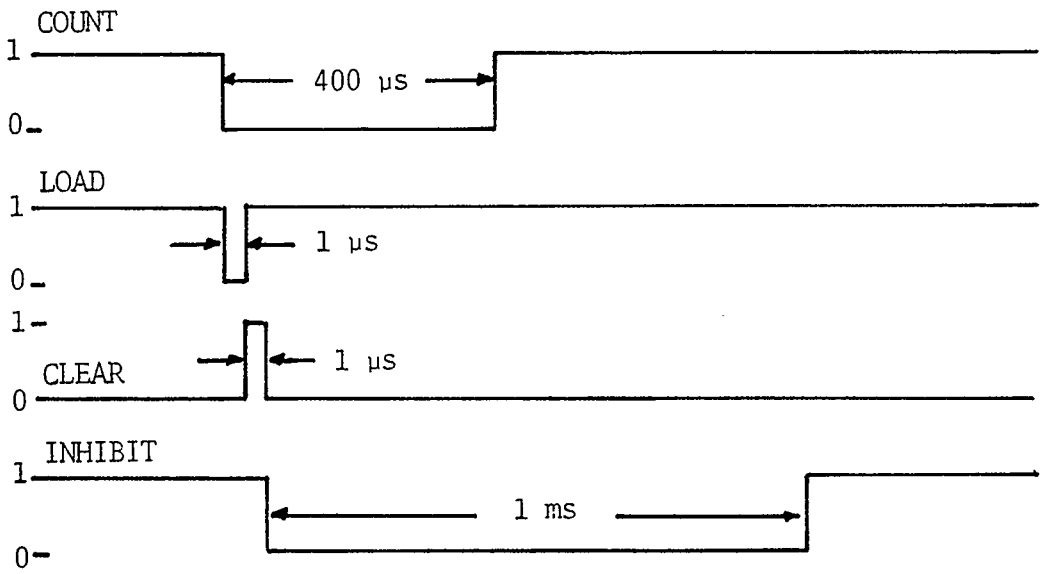

Fig. 5.1(b) Timing diagram of Fig. 5.1(a).

The opto-coupler acts as a switch that allows the counters to count up when exposed to light and inhibits counting when it is not exposed to light. By rigidly attaching a tab to a plate on the end of the dc machine shaft in Fig. 2.1, the angular rotation of a rotor shaft is used to control the operation of the circuit in Fig. 5.1(a). The tab is used to interrupt the light exposing an opto-coupler once every revolution. The width of the tab determines how long the opto-coupler inhibits the counting.

A timing diagram of the circuit in Fig. 5.1(a) is shown in Fig. 5.1(b). Whenever light falls on the photo-diode, the circuit counts. But as soon as the tab inhibits the light, the counting is stopped and the value of the counters is loaded into the output buffer. After loading the output buffer the contents of the counters are reset to zero with a clear pulse. The clear pulse causes an inhibit signal to trigger. The purpose of this is to inhibit the retriggering of the load and clear pulses when the photo-diode turns on again.

The output buffer can be loaded directly into the computer. The speed estimate is contained on all 16 lines of the computer input buffer. In order to compare the effect of the clock rate on the measurement technique, a provision has been made for four different clock rates by dividing the 1 MHz clock down to: 500, 250, 125 and 62.5 kHz.

5.2.2 Waveform Sampling Technique

A block diagram of the laboratory setup used to apply this technique is shown in Fig. 5.2. This set uses the micro-machine that is used for the encoder technique. A tach is coupled to the same end of the rotor as the encoding disc.

The ac voltage signal generated by the tachogenerator is attenuated by a rheostat and filtered by a sixth order bandpass filter with a passband that was set between 30 and 90 Hz. After filtering, the signal goes to the data acquisition system where it is digitized with a 12 bit A/D converter. The speed measurement algorithm in the computer processes the most recent sample and then waits until the next sample has been converted. The sample rate is controlled externally with a pulse generator.

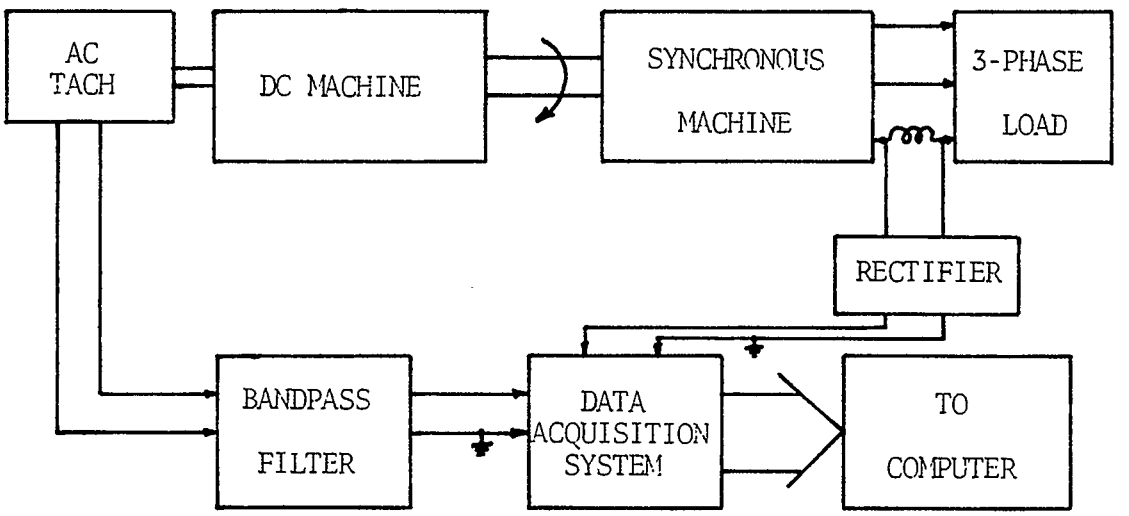

Fig. 5.2 Block diagram of laboratory setup of waveform sampling technique.

5.3 RESULTS OF STATIC TESTS

5.3.1 Description of Static Test

A static test is performed by estimating the frequency of a constant signal. This makes possible the observation of the resolution of the technique being used. For the static tests the speed signal from the micro-machine is simulated with a pulse generator or a frequency synthesizer depending on the technique.

The top waveform in Fig. 5.1(b) is the signal from the opto-coupler that controls the operation of the circuit in Fig. 5.1(a). This waveform can be simulated with a pulse generator. The period of the pulse generator is controlled externally with a high precision clock. The waveform sampling technique samples a sinusoidal signal to produce the estimates. A sinusoidal waveform like that generated by a tach can be reproduced with a frequency synthesizer.

5.3.2 Results from the Static Test

Static tests are performed by making 200 consecutive measurements with the clock or the frequency synthesizer set at a desired value. After the measurements were made the data was normalized and recorded on a digital plotter.

5.3.2.1 Constant-displacement shaft-encoder

All tests applying this technique were made using two different clock frequencies for the counters: 62.5 and 500 kHz. The results of the tests for each clock rate are shown in Figs. 5.3 and 5.4 respectively. Each figure has two plots; the upper plot illustrates the results of frequencies within ±0.1 Hz of 60 Hz and the lower plot illustrates the results of frequencies within ±2.4 Hz of 60 Hz. The

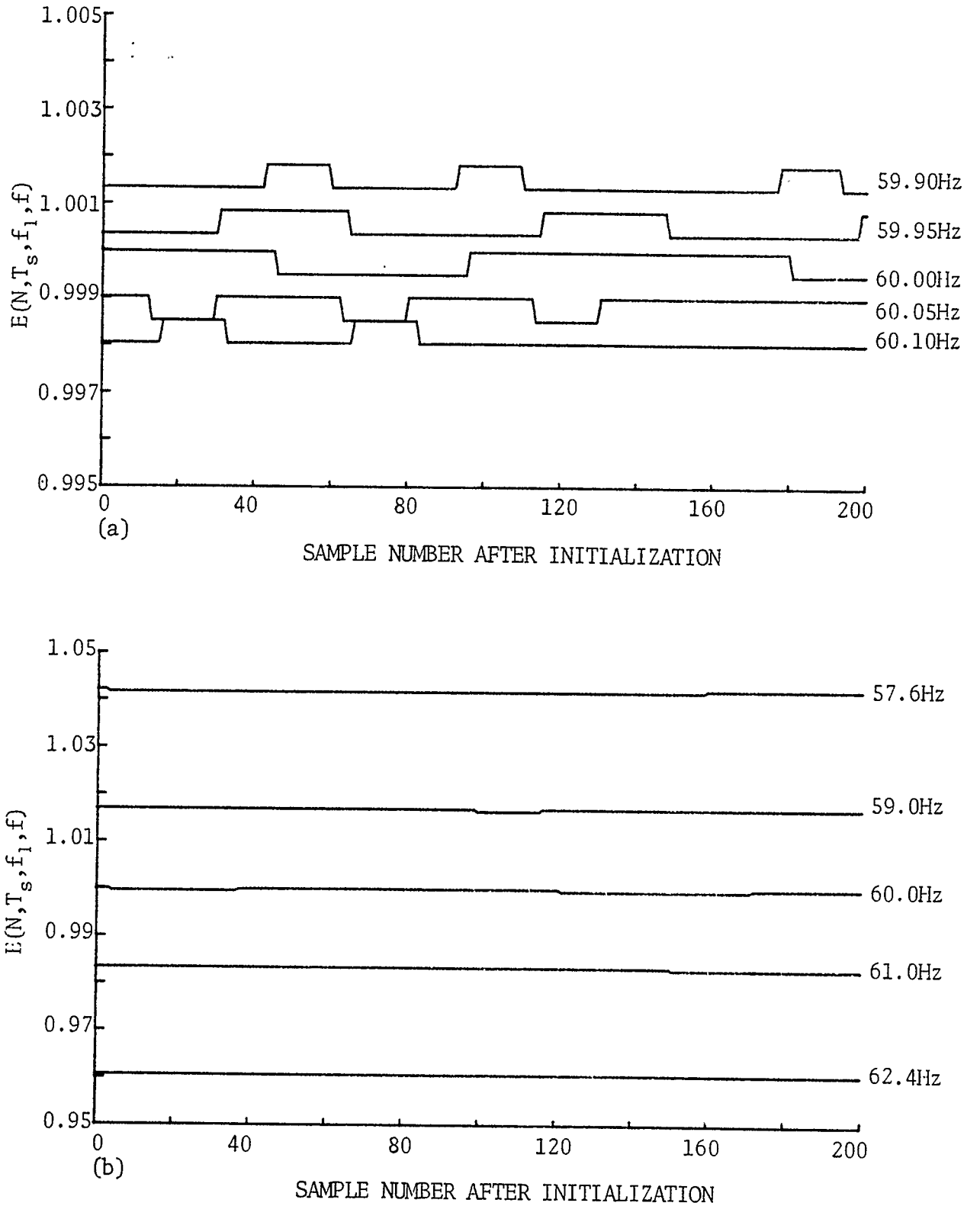

Fig. 5.3 Shaft-encoder static tests. Clock rate equal to 62.5 kHz.

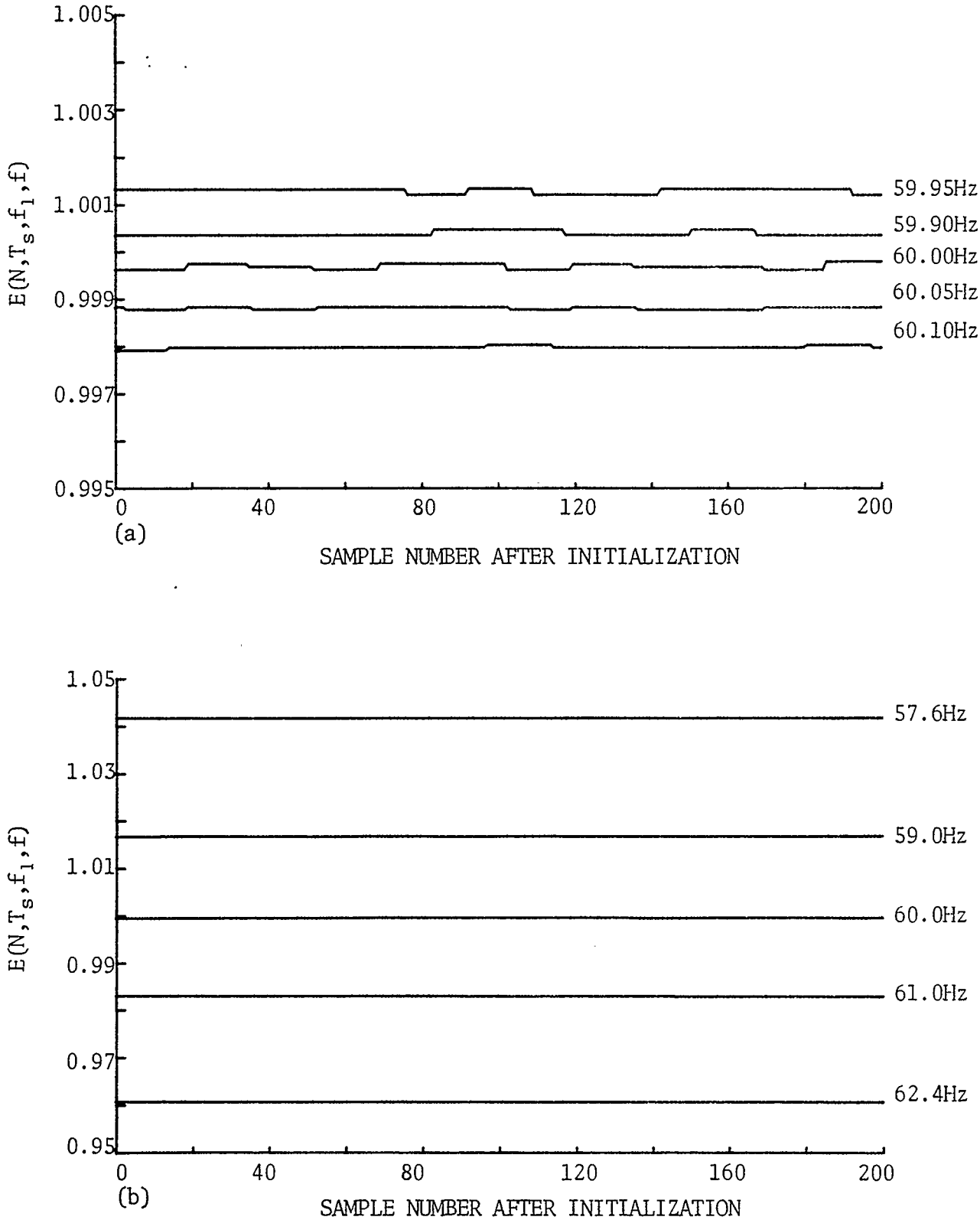

Fig. 5.4 Shaft-encoder static tests. Clock rate equal to 500 kHz.

lower graph corresponds to the maximum speed range of a turbine-generator. The horizontal axis represents the time of the estimate. The length of time required for each test is not the same because the time required for an estimate depends on the frequency of the signal. The vertical axis is the value of the estimate.

As seen in Figs. 5.3(a) and 5.4(a), the estimates of each frequency result in two distinct upper and lower values. These are tabulated in Table II along with the maximum difference between the estimates and the theoretical value of the estimate. Eqn. (2.8) in Chapter 2 states that the mean error of the speed estimate will decrease proportionately with an increase in the clock rate. Table II and Figs. 5.3(a) and 5.4(a) show that the error does decrease as the clock rate increases. However, the clock rate increased by a factor of 8 and in only one case did the error decrease by 8. Also, the mean error from eqn. (2.8), for a clock rate of 62.5 kHz, is 0.024%. The maximum error is twice this value, or 0.048%. Table II shows that this is the error observed when the clock rate is 62.5 kHz.

Theoretically this ensures a resolution of 0.03 Hz. Fig. 5.3(a) shows that the estimate of 60.05 Hz coincides with the estimate of 60.1 Hz, which implies that the resolution is greater than 0.05 Hz, or that the clock used to generate the 60.05 Hz signal is not true. The maximum theoretical error at a clock rate of 500 kHz is 0.006% which is indicated only once in Table II. Since the other errors are larger and not consistent, an effect other than quantization must be affecting the data. Again, this could be due to frequency drift of the clock used to generate the test signals.

TABLE II SHAFT-ENCODER RESOLUTION

CLOCK RATE OF 62.5 kHz

FREQUENCY Hz	THEORETICAL ESTIMATE p.u.	LOWER ESTIMATE p.u.	UPPER ESTIMATE p.u.	DIFFERENCE p.u.
59.90	1.00170	1.00146	1.00194	0.00048
59.95	1.00083	1.00049	1.00097	0.00048
60.00	1.00000	0.99951	1.00000	0.00049
60.05	0.99917	0.99854	0.99903	0.00049
60.10	0.99830	0.99806	0.99854	0.00048

CLOCK RATE OF 500 kHz

59.90	1.00170	1.00128	1.001466	0.000186
59.95	1.00083	1.00043	1.00055	0.00012
60.00	1.00000	0.99964	0.99982	0.00018
60.05	0.99917	0.999879	0.99885	0.00006
60.10	0.99830	0.99793	0.99806	0.00013

5.3.2.2 Waveform sampling technique

Static tests applying this technique were made using a reference frequency of 40 Hz and weights of N=15 and N=18. This corresponds to sampling rates of 600 and 720 Hz respectively. Tests were performed in exactly the same manner as for the shaft-encoder technique. But in this case a frequency synthesizer was used to simulate the speed signal. The results are illustrated in Figs. 5.5 and 5.6.

The estimates on these graphs are normalized to 1, but will result in different values than those corresponding to similar estimates made for the encoding technique. The reason for this is shown in Fig. 4.8 of Chapter 4, which displays the theoretical estimate for each frequency in the range of interest. As can be seen in Fig. 4.8, a change in frequency of 4% corresponds to a change in the estimate of 25%, so an estimate of 1.25 per unit corresponds to a frequency which is 4%

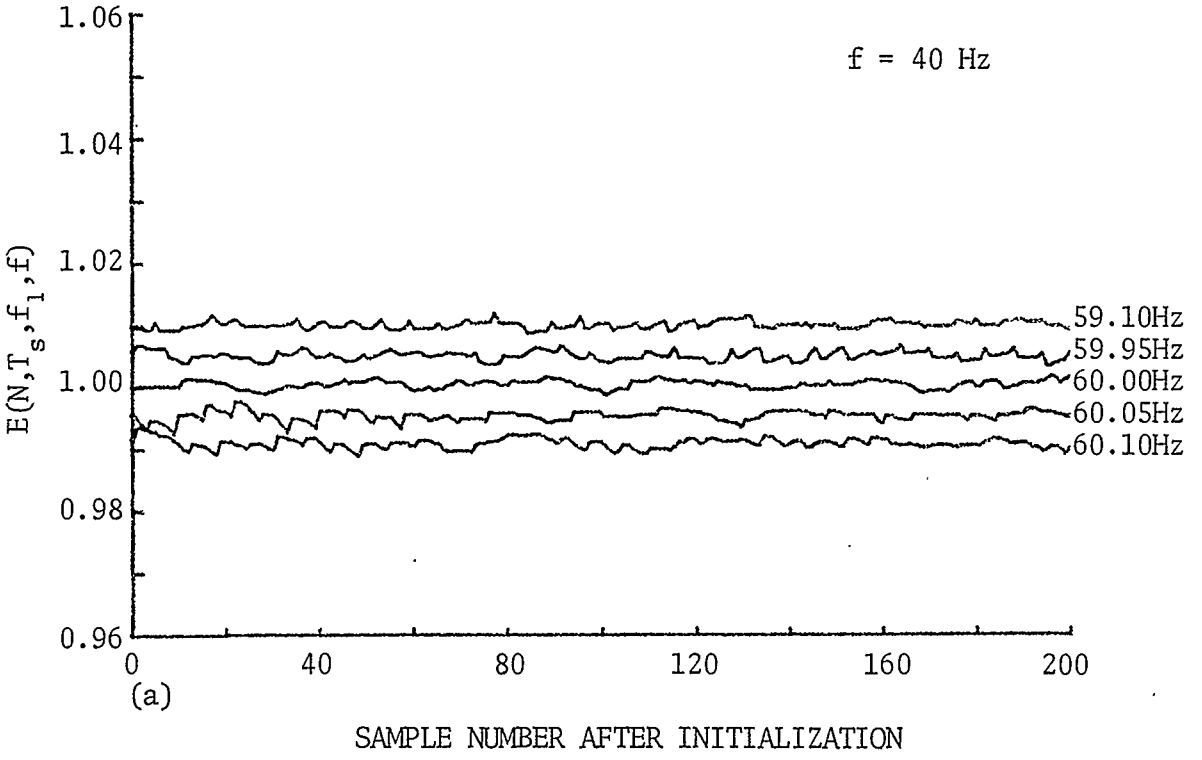

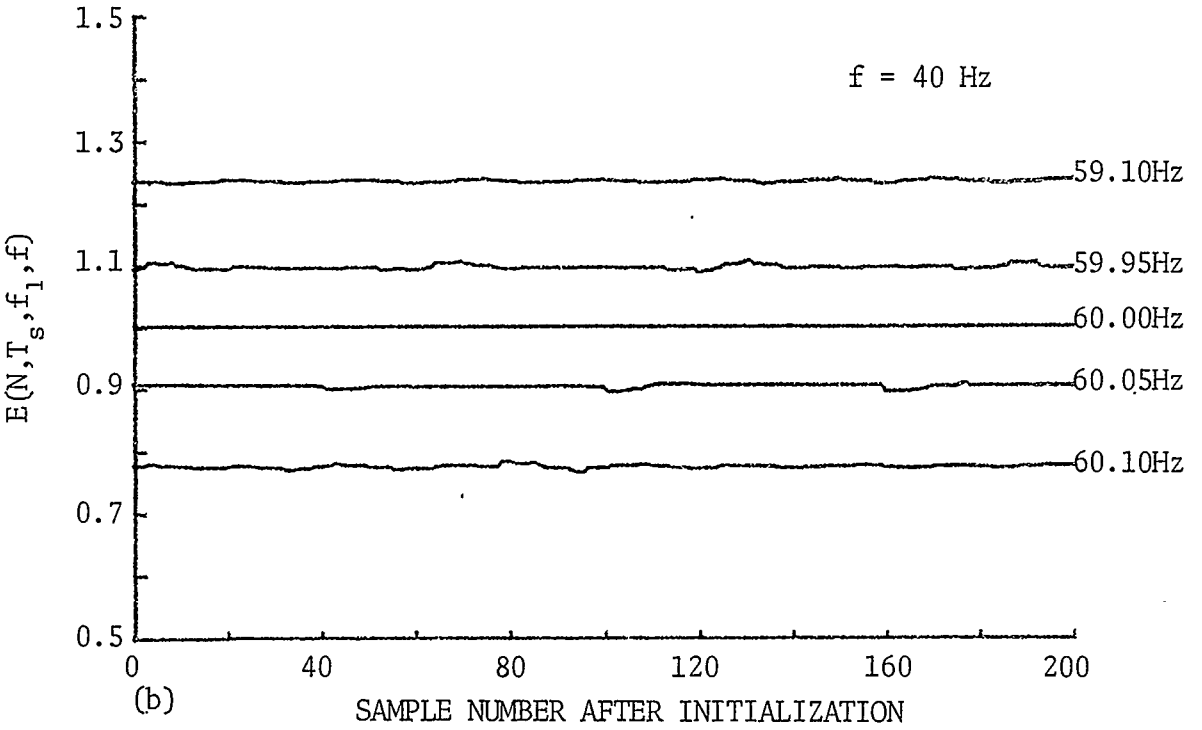

Fig. 5.5 Waveform sampling static tests. N = 15.

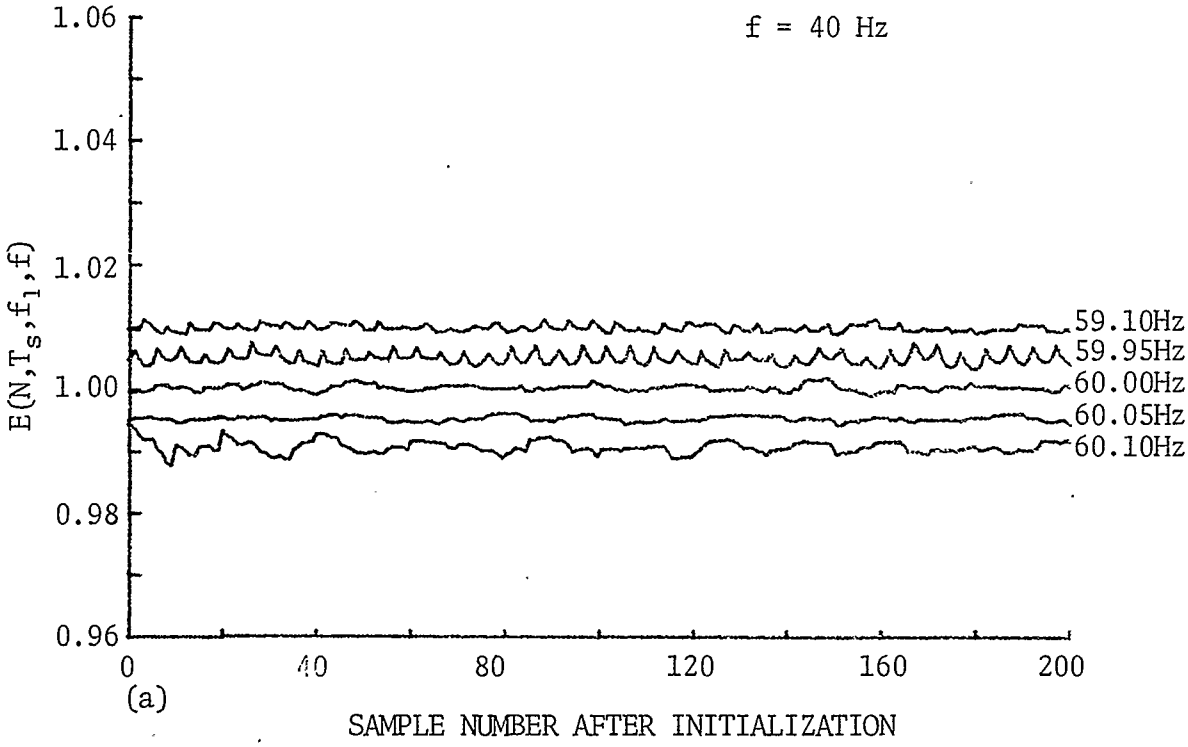

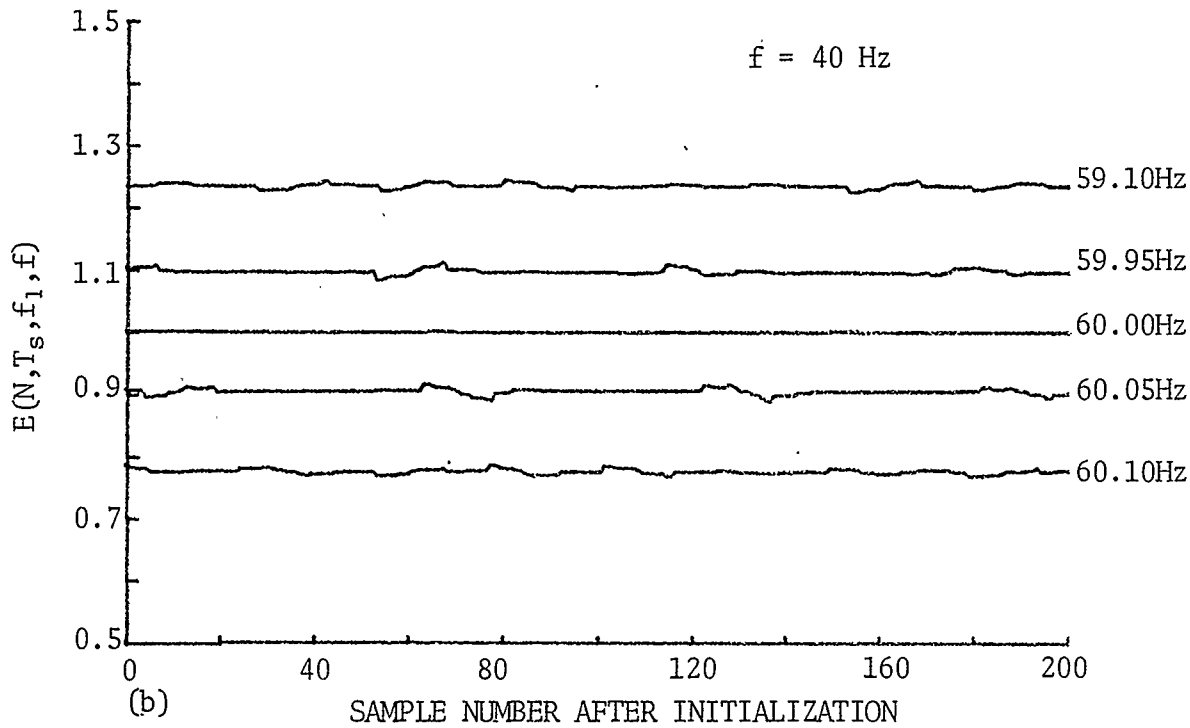

Fig. 5.6 Waveform sampling static tests. N = 18.

less than 60 Hz.

Figs. 5.5(a) and 5.6(a) show that a resolution of 0.05 Hz is possible because the estimates of 59.9, 59.95, 60 and 60.05 Hz are distinct. However, the algorithm was found to be sensitive to the amplitude of the signal.

The derivation of the waveform sampling technique in Chapter 3 assumed that an orthogonal pair of sinusoids were available. In Chapter 4 it was stated that one signal of the orthogonal pair must be calculated from samples of the only sinusoidal signal that was available. Because of this, the amplitude of the sampled signal must be assumed to be constant. If this is not true then eqns. (3.24) and (3.25) will be weighted by different values of the amplitude, so the phase dependent terms will not cancel. This results in adding a term to the estimate that oscillates at twice the frequency of the sampled signal.

A very definite indication of the sensitivity to amplitude is illustrated in Fig. 5.6(a). The estimate of 59.95 Hz has a definite periodic oscillation. There are about four peaks of this oscillation for every 18 samples or one cycle of the measured signal. If the amplitude has a slight error the effect of this error is most apparent at the positive and negative maximums of the signal or twice for every cycle. This effect appears as a double frequency signal and this results in the ripple that is observed on the estimate.

Comparing Figs. 5.5(a) and 5.6(a), there does not appear to be an increase in resolution by increasing the number of samples used for an estimate. This is demonstrated by Fig. 4.8 which plots the lines for estimates at different values of N. As N increases, the slopes of these lines do not increase appreciably; thus the resolution will not

increase to any great extent.

5.4 DYNAMIC TESTS

5.4.1 Description of the Tests

Dynamic tests were performed using the micro-machine setup illustrated in Fig. 5.2. The results of four tests are plotted in Figs. 5.7 to 5.10. These tests are dynamic because the speed of the micro-machine changes from one value to another while measurements are being made.

Connecting the correct value of load to the generator could change the speed from rated value to 2 or 4% greater than rated. This is accomplished by switching resistors in parallel to act as a change in load. Figs. 5.7 and 5.9 correspond to a 2% change in speed, and Figs. 5.8 and 5.10 correspond to a 4% change in speed.

On all the graphs, 600 samples are displayed along the horizontal axis.

Each test was performed by taking 1000 samples at constant speed. After the 1000 samples, the program applying the techniques simultaneously will continue sampling but consecutive estimates are no longer stored. There is a delay on each graph that illustrates the initial condition which existed before the speed changed. After the load changes and during the interval that the micro-machine accelerates to the new speed value, 11000 samples are taken. This is enough time for the algorithm to settle to a new steady state speed.

The change in load is sensed by monitoring the rectified output of a current transformer connected in one of the phases. When the load is changed, this quantity will change almost instantaneously with

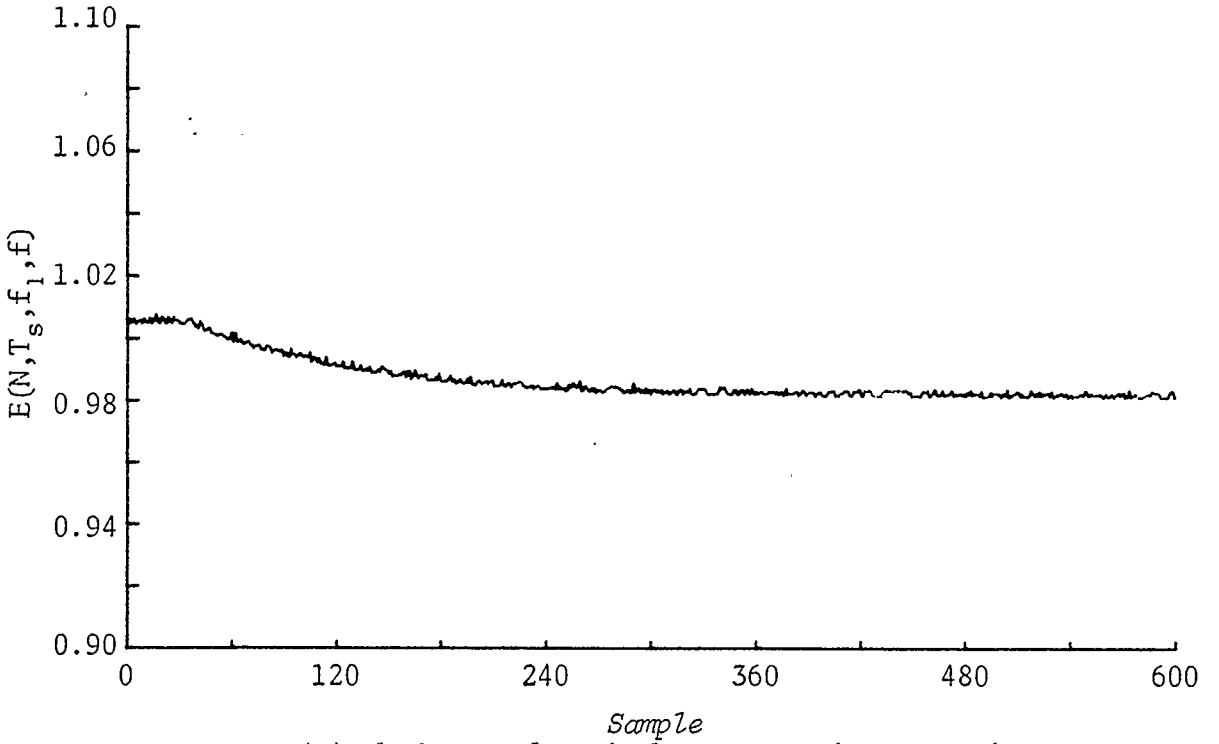

(a) Shaft-encoder clock rate equal to 62.5 kHz.

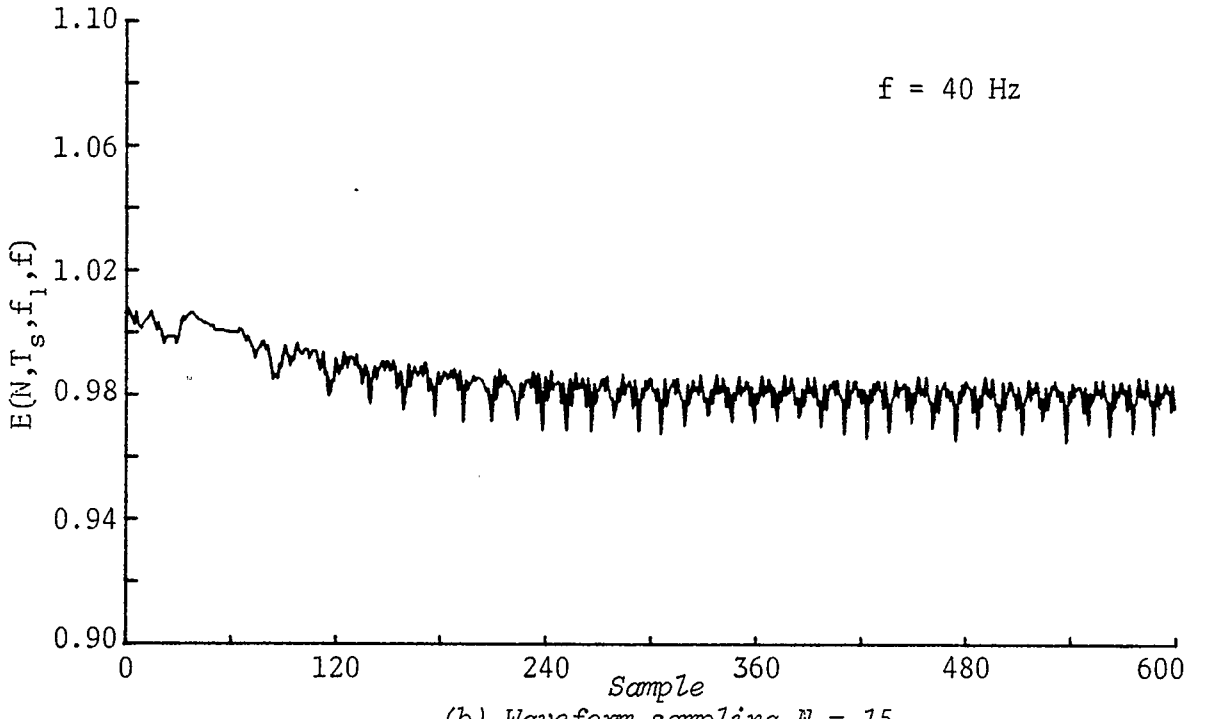

(b) Waveform sampling N = 15.

Fig. 5.7 Dynamic tests 2% change in speed.

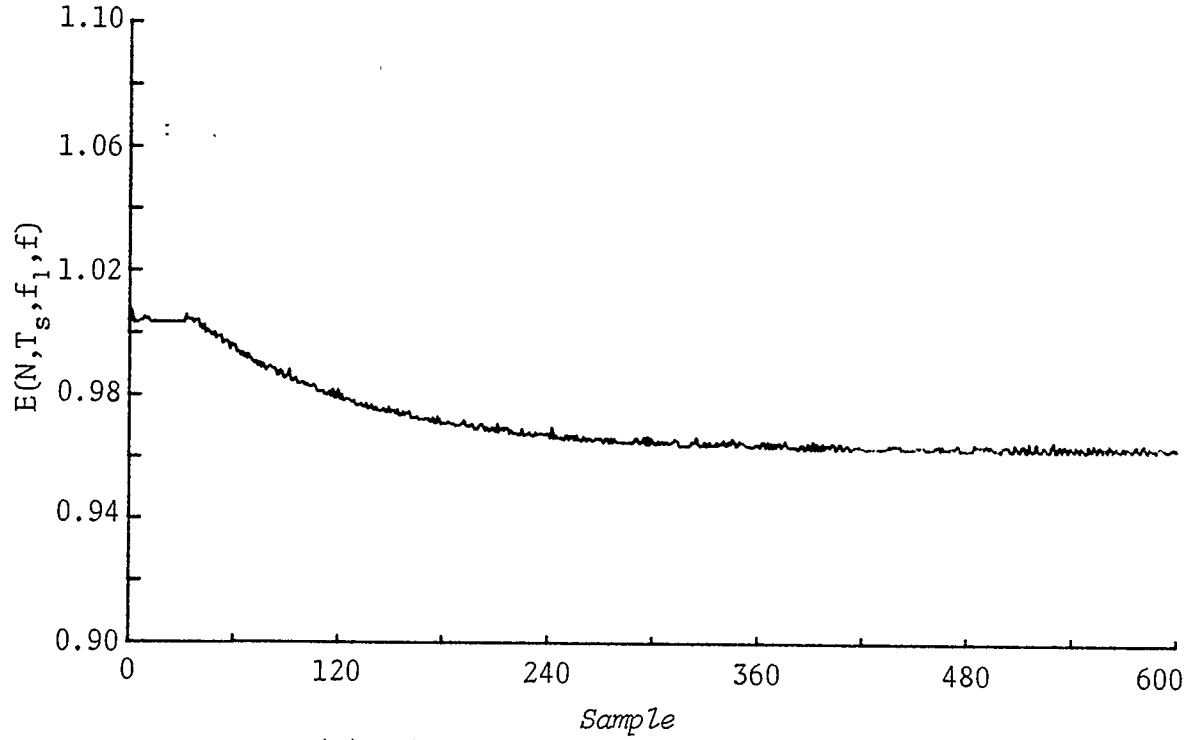

(a) Shaft-encoder clock rate equal to 62.5 kHz.

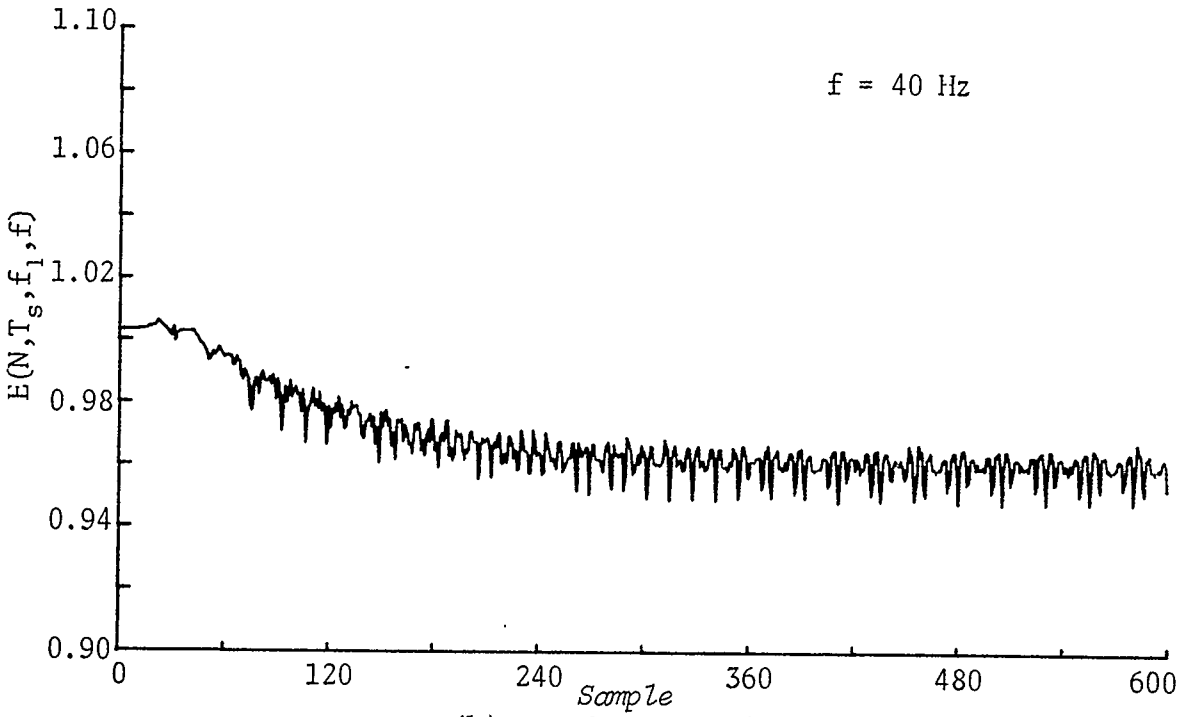

(b) Waveform sampling N = 15.

Fig. 5.8 Dynamic tests 4% change in speed.

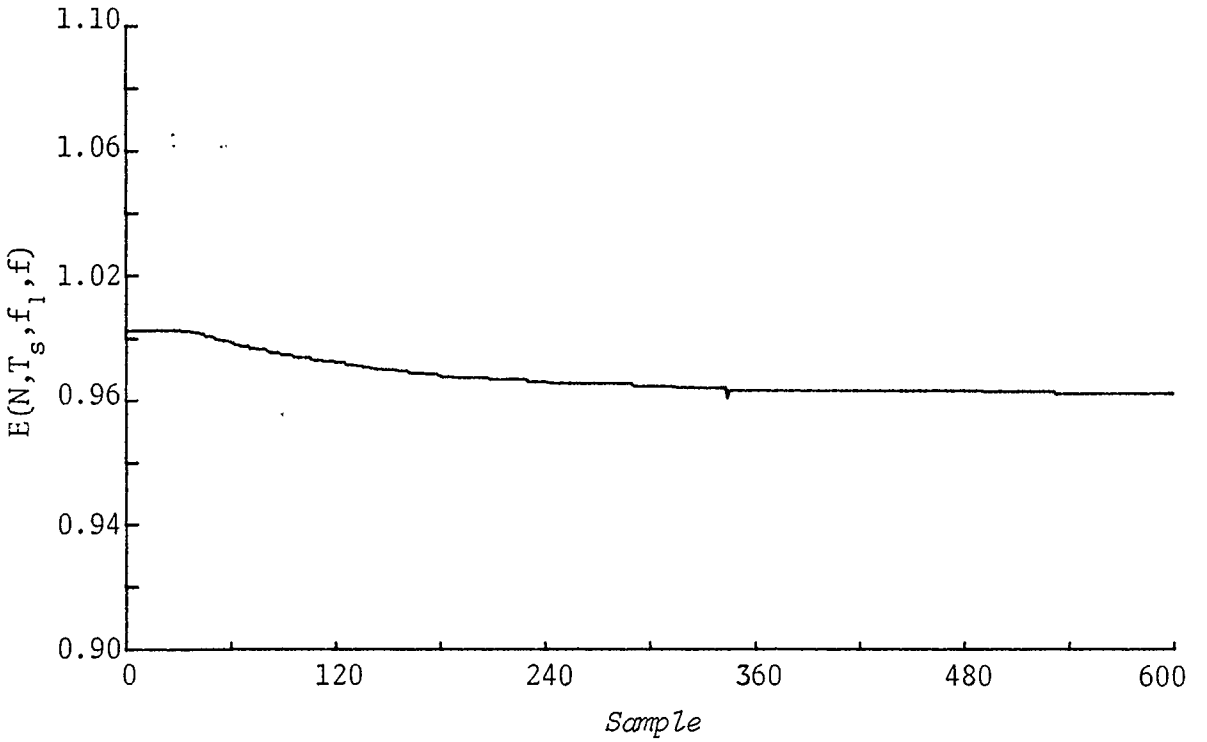

(a) Shaft-encoder clock rate = 500 kHz.

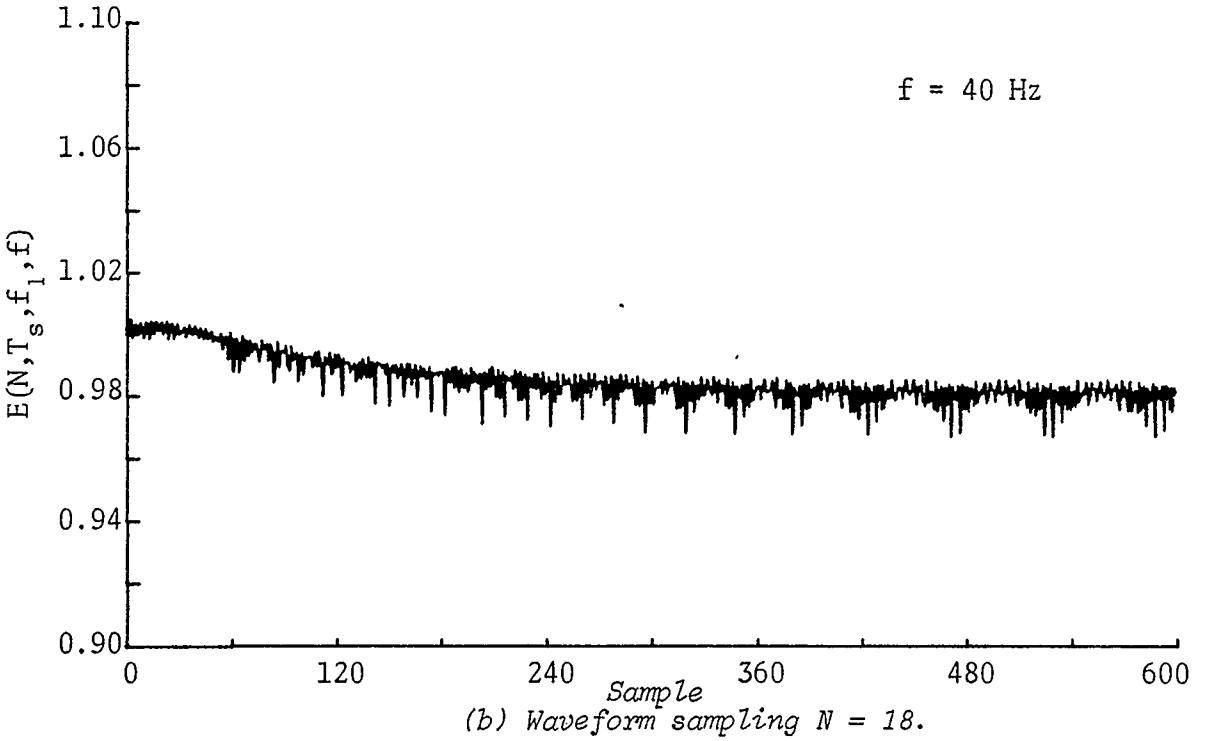

(b) Waveform sampling N = 18.

Fig. 5.9 Dynamic tests 2% change in speed.

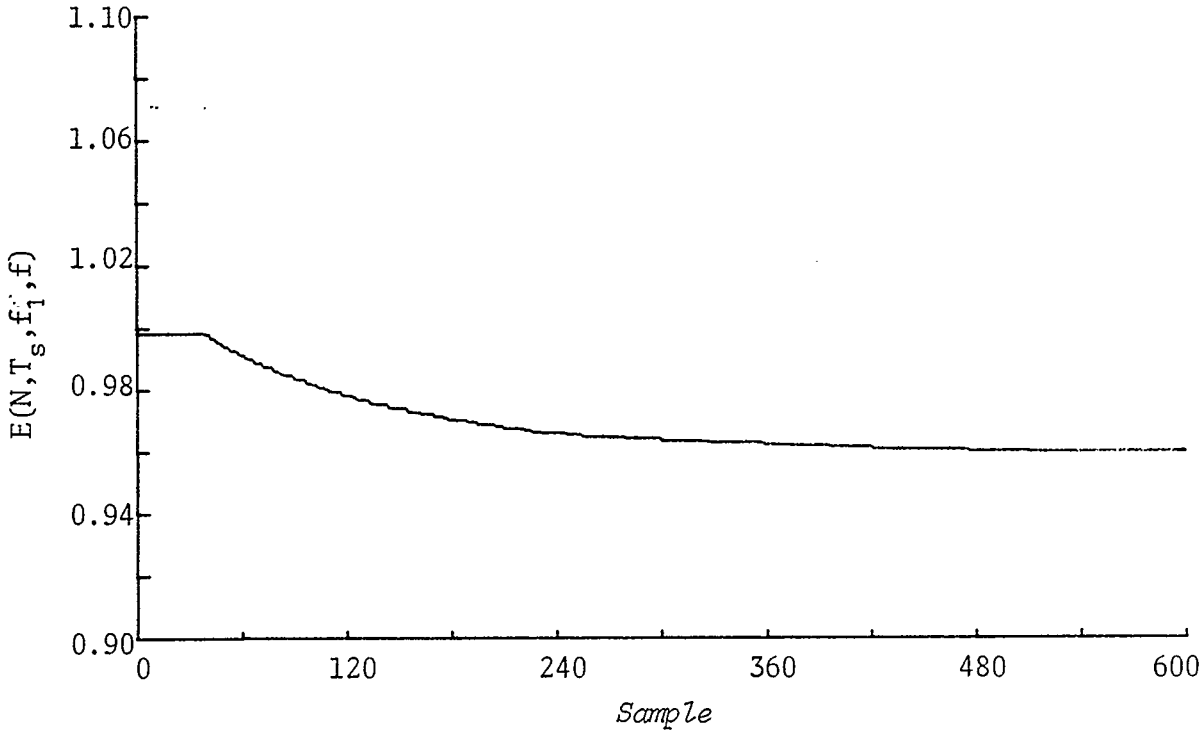

(a) Shaft-encoder clock rate equal to 500 kHz.

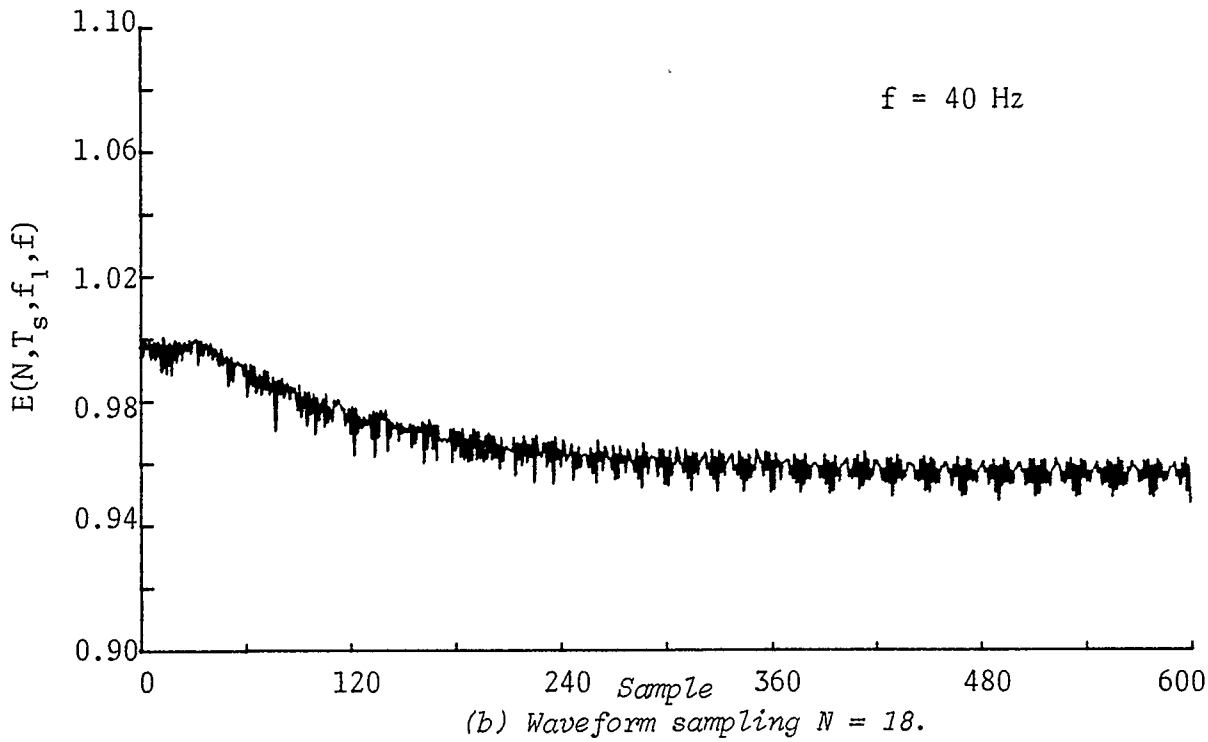

(b) Waveform sampling N = 18.

Fig. 5.10 Dynamic tests 4% change in speed.

respect to a change in speed of the shaft, because the electrical time constant of the load is much less than the mechanical time constant of the rotor.

A sample of both techniques is made simultaneously. One sample of the shaft-encoder technique corresponds to the most recent estimate of the speed of the rotor, while one sample of the waveform sampling technique is processed with the N-1 most recent samples to produce an estimate.

The shaft-encoder technique will update once every revolution or about 33 ms, so many of the samples taken will have the same estimate. This is because the sampling rate is determined by the waveform sampling technique and is much faster than 33 ms. However, due to the large number of samples acquired during the test, only some of them can be saved. So every 20th estimate made is stored. Therefore, Figs. 5.7 to 5.10 display only 600 samples of the estimates.

Since N is larger in Figs. 5.9 and 5.10, the sampling rate used for this data is faster. Therefore, the total time for these tests is less than that for the tests using N=15. In Figs. 5.7 and 5.8 the time between hatchmarks is 2 seconds after the load has changed, and in Figs. 5.9 and 5.10 the time is 1.67 seconds.

5.4.2 Results

5.4.2.1 Constant-displacement shaft-encoder

Comparing Figs. 5.7(a) and 5.8(a) to Figs. 5.9(a) and 5.10(a), the quantization error from the time measurement decreases as the clock rate is increased. All four tests follow the change in speed well.

Fig. 5.9a has one bad estimate at about the 350th plotted point. This is most likely due to the design of the part of the encoder circuit that transfers data from the counters to the output buffer. If the computer attempts to make a sample when the transfer is taking place, an invalid sample would occur because the state of the output buffer at this time is undefined.

5.4.2.2 Waveform sampling

If the upper graph is superimposed on the lower graph in all four figures, the estimate of the shaft-encoder falls directly along the heaviest part of the area of estimates from the waveform sampling technique.

Before the transient occurs the estimate of rated speed is stable. But as soon as the load changes the estimate begins to oscillate. At the new steady state value the estimate oscillates about 2% in value. Again this error can be attributed to the change in amplitude of the signal from the tach. This technique follows the change in speed well.

5.5 CONCLUSION

Static and transient tests have been performed on the constant displacement shaft-encoder technique and the waveform sampling technique. Static tests indicate that a resolution of 0.05 Hz is possible with both techniques. The error in the shaft-encoder technique is decreased as the clock rate of the counters is increased.

A double frequency signal is introduced onto the estimate of the waveform sampling technique if the amplitude of the signal is not known exactly by the algorithm.

Transient tests show that both techniques can follow a change in the speed of a rotor shaft. However, the error in the waveform sampling technique increases as the speed changes because the amplitude of the signal generated from the tach also changes with speed.

CHAPTER 6

DISCUSSION AND RECOMMENDATIONS

The objective of this work is to develop a new digital technique of measuring the angular speed of a turbine-generator unit. It is required that the speed be measurable to a resolution of 0.01% and the estimate of the speed should update once every 25 ms. High resolution like that specified is a requirement of modern power systems. Implementation of direct digital control to turbine-generator units needs a speed estimate that updates this rapidly.

6.1 WAVEFORM SAMPLING TECHNIQUE

A digital technique of measuring angular speed is proposed in this thesis. The basis of this method is a waveform sampling technique that uses the information contained in the amplitude of a sinusoidal signal to estimate the frequency of oscillation of the signal. An ac tachogenerator generates a sinusoidal voltage at a frequency proportional to the speed of its rotor. Therefore, by coupling a tachogenerator to the shaft of a turbine-generator unit, the waveform sampling technique can be used to estimate the angular speed of the turbine-generator. The details of the derivation and the implementation of this technique are described in Chapters 3 and 4 respectively.

Static and transient tests on this technique are described in detail in Chapter 5. Under steady state conditions a resolution of 0.05 Hz or 0.08% is possible. But under dynamic conditions the

resolution deteriorates to 2%. These results are illustrated in Figs. 5.7 to 5.10. As can be seen, the calculated value of the estimate in the static tests oscillates around an average value. The reason for this oscillation is discussed below.

Three static tests at three different frequencies are illustrated in Fig. 6.1. The magnitude of the oscillation is large enough to reduce the resolution to 0.1 Hz or 0.167%. The simulation of this oscillation was caused by introducing a 1% error in the amplitude of the direct signal. It can be seen that the technique is sensitive to errors in the amplitude of the signals being measured.

6.2 CONSTANT-DISPLACEMENT SHAFT-ENCODER

The shaft-encoding techniques discussed in Chapter 2 are capable of performance requirements similar to those of the waveform sampling method. There are two types of encoding techniques. One requires an encoding disc with more than 1000 holes and the other requires an encoder with one or two holes if the requirements for the waveform sampling technique are to be met. The second method was applied to the same speed measurement problem as the waveform sampling technique. The first method was not considered because the construction of an encoding disc with 1000 precisely spaced holes around its perimeter would have been an impractical undertaking.

The results from the static and dynamic tests on the shaft-encoder show that this method can achieve a high resolution and has a satisfactory transient response. The static test results illustrated in Figs. 5.3 and 5.4 show that a resolution of better than 0.05 Hz is possible. The angular velocity of the shaft determines how often the

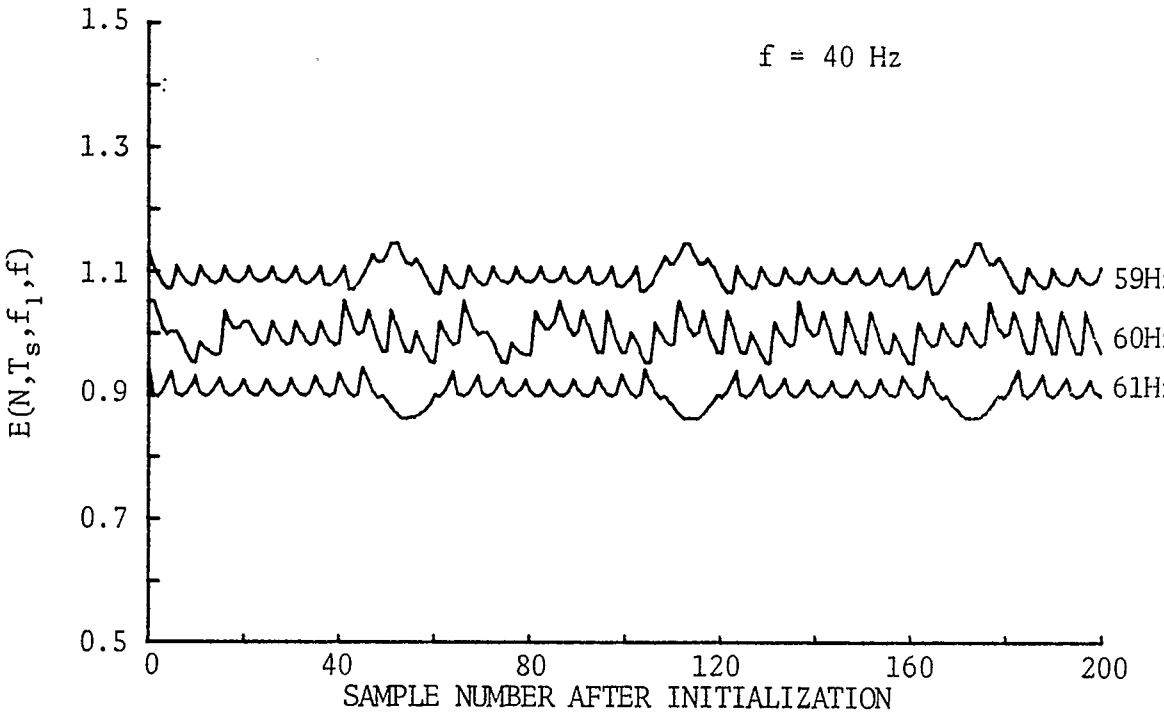

Fig. 6.1 Simulation of a 1% error in the amplitude of the direct signal N = 15.

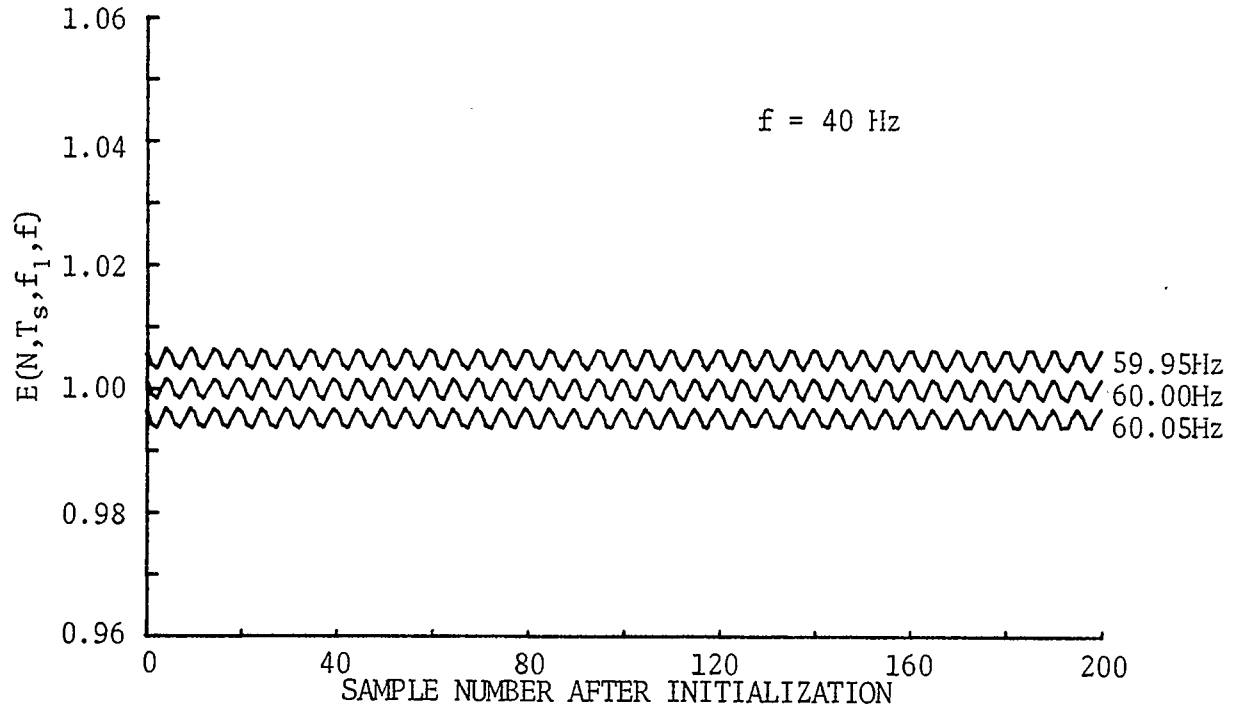

Fig. 6.2 Simulation of a 0.5° error in phase between direct and quadrature signal N = 15.

estimate updates because this technique measures time per unit displacement. Therefore, if the angular velocity of the turbine-generator unit is 1800 rpm, this estimate will update once every 33 ms.

The shaft-encoder technique has the following disadvantages:

i) The photo-diode requires an intense light source to operate properly. If the source is displaced with respect to the photo-diode, there will be an insufficient amount of light, resulting in the diode working intermittently or not at all.

ii) The light source has a finite lifetime; thus requires periodic replacement.

iii) The estimate of vibrations on the shaft will not change linearly with shaft speed. This is illustrated by Fig. 2.6. These vibrations will not affect the waveform sampling technique because the bandpass filter eliminates them.

Estimation of oscillations on the shaft can be improved if more than one term of the Taylor series expansion given by eqn. (2.10) were utilized for the speed estimation. This has been attempted in reference 26, where the authors are measuring the frequency of a power system.

6.3 RECOMMENDATIONS

The performance of the waveform sampling technique can be improved by using a two-phase tachogenerator instead of a single-phase tachogenerator. If this type of tachogenerator is used the amplitudes of the two generated signals are likely to be equal. This can be taken advantage of to increase the sensitivity of the algorithm. Also, an orthogonal signal no longer need be calculated from the direct signal. Therefore, the errors that are present in Fig. 6.1 will not occur

because these came from the assumption that the amplitude of the direct signal would remain constant.

Application of a two-phase tachogenerator relies upon the generated signals being exactly 90° out of phase. This relationship can be verified experimentally to a resolution of 0.5°. Fig. 6.2 illustrates the simulation of the estimates of three frequencies which are 0.05 Hz apart and which have a 0.5° error between the direct and quadrature signals that form the orthogonal pair. As in Fig. 6.1, a double frequency oscillation occurs as a result of the phase error. However, in this case the amplitude of the oscillation is less, so a higher resolution is possible.

Due to the length of the algorithm written for speed measurement, this technique requires the performance of a high-speed minicomputer. The cost of a minicomputer makes the application of this method impractical. Therefore this technique must be applied with the relatively inexpensive and slower microprocessor. The central processing unit of a microprocessor runs an order of magnitude slower than that of a minicomputer. Roughly speaking, the execution time on a microprocessor is expected to be of the order of 10 ms. Thus the algorithm and the implementation of this technique must be more efficient with the use of time if sample rates of 600 to 720 samples per second are to be attained.

Use of a two-phase tachogenerator results in a smaller program with decreased execution time because the subroutines required to generate an orthogonal signal are not required. Another reason for the long execution time is the use of floating point instructions for calculations. If integer instructions are used, a calculation will

take less time. Alternatively, with the use of a hardware multiplier the execution time would drop considerably. The form of the algorithm lends itself to application with more than one microprocessor. The estimate at each sample interval is the sum of four identical and independent calculations. If each calculation was performed on one microprocessor, the execution time is immediately reduced to one fourth. With these suggestions the execution time should drop to within the capabilities of a microprocessor, which results in an economic and practical application of the waveform sampling technique.

REFERENCES

1. W. D. Stevenson Jr., *Elements of Power Systems Analysis*, McGraw-Hill, 1975.
2. O. I. Elgerd, *Electric Energy Systems Theory*, McGraw-Hill, 1974.
3. *Better Control of Electric Power Systems*, Publication of the Energy Research and Development Administration, Washington, 1977.
4. D. W. Huber, "Real-time DAVR for a generating unit," Ph.D. Thesis, University of Calgary, 1974.
5. A. A. El-Ghandakly, "On-line adaptive control of a generating unit," Ph.D. Thesis, University of Calgary, 1975.
6. A. A. Ramanujam, "Modal reference adaptive control," M.Sc. Thesis, University of Calgary, 1977.
7. G. Hoffmann de Visme, "Digital processing unit for evaluating angular acceleration," *Electronic Engineering*, pp. 183-188, April 1968.
8. K. K. Oey, R. J. Thomas, "A digital technique for measurement of speed deviation and torque angle during the transient interval," presented at Canadian Communications and Power Conference, 1976.
9. M. M. Elmetwally, "Low sensitivity control of power systems," Ph.D. Thesis, University of Calgary, 1974.
10. D. W. Huber, O. P. Malik, G. S. Hope, "A digital device to measure angular speed and torque angle," *IEEE Transactions of Industrial Electronics and Control Instrumentation*, vol. IECI, No. 2, May 1975.
11. B. Szabados, N. K. Sinha, C. D. DiCenzo, "A new digital instrument for measuring angular velocity and acceleration," *Proceedings of the IEEE*, pp. 455-456, vol. 60, April 1972.

12. C. D. DiCenzo, B. Szabados, N. K. Sinha, "Digital measurement of angular velocity for instrumentation and control," *IEEE Transactions on Industrial Electronics and Control Instrumentation*, vol. IECI-23, No. 1, Feb. 1976.

13. D. F. Hoeschele Jr., *Analog-Digital/Digital-Analog Conversion Techniques*, John Wiley and Sons, 1968.

14. R. P. Moffat, P. Bhartia, "Electromagnetic instrumentation for rotational machinery monitoring and control," University of Regina.

15. K. N. Stanton, "Analysis of interconnected power systems using normal operating data," Ph.D. Thesis, University of New South Wales, 1964.

16. A. Dunworth, "Digital instrumentation for angular velocity and acceleration," *IEEE Transactions on Instrumentation and Measurement*, vol. 18, No. 2, June 1969.

17. L. R. Rabiner, B. Gold, *Theory and Application of Digital Signal Processing*, Prentice-Hall Inc., 1975.

18. A. V. Oppenheim, R. W. Schafer, *Digital Signal Processing*, Prentice-Hall Inc., 1975.

19. A. Papoulis, *Probability Random Variables and Stochastic Processes*, McGraw-Hill, 1965.

20. M. E. Van Valkenburg, *Network Analysis*, Prentice-Hall Inc., 1974.

21. E. O. Brigham, *The Fast Fourier Transform*, Prentice-Hall Inc., 1974.

22. R. W. Hamming, *Digital Filters*, Prentice-Hall Inc., 1977.

23. A. E. Fitzgerald, C. Kingsley Jr., A. Kusko, *Electric Machinery*, 3rd ed., McGraw-Hill Book Company, Toronto, 1971.

24. B. M. Weedy, *Electric Power Systems*, John Wiley and Sons, 2nd ed., 1972.

25. D. H. Thorne, E. F. Hill, "Field testing of hydraulic turbine governor performance," presented at the IEEE PES Summer Meeting and EHV/UHV Conference, March 1973.

26. M. S. Sachdev, M. M. Giray, "A digital and rate of change of frequency relay," presented at the System Planning and Operation Section Spring Meeting, CEA, March 1978.

APPENDIX I

DERIVATION OF THE FOURIER TRANSFORM OF EQUATION (3.7)

Equation (3.1) and the definition of the Fourier Transform of a discrete time sequence are repeated as eqns. (A.1) and (A.2) respectively.

$$x_T(kT_s) = \begin{cases} cos(2\pi f_1 kT_s + \psi), & 0 \le k < N \\ 0, & \text{elsewhere} \end{cases} \tag{A.1}$$

$$X_T(e^{j2\pi fT_s}) = \sum_{k=-\infty}^{\infty} x_T(kT_s)e^{-j2\pi fkT_s}. \tag{A.2}$$

Since eqn. (A.1) is equal to zero for k less than zero or greater than or equal to N, the Fourier Transform of eqn. (A.1) may be written as,

$$X_T(e^{j2\pi fT_s}) = \sum_{k=0}^{N-1} cos(2\pi f_1 kT_s + \psi)e^{-j2\pi fkT_s}. \tag{A.3}$$

Writing the cosine function in terms of exponentials gives

$$X_T(e^{j2\pi fT_s}) = \frac{1}{2}\sum_{k=0}^{N-1} [e^{j(2\pi f_1 kT_s+\psi)} + e^{-j(2\pi f_1 kT_s+\psi)}]e^{-j2\pi fkT_s} \tag{A.4}$$

Multiplying through with the common exponential term gives

$$X_T(e^{j2\pi fT_s}) = \frac{1}{2}\sum_{k=0}^{N-1} [e^{j(2\pi kT_s(f_1-f)+\psi)} + e^{-j(2\pi kT_s(f_1+f)+\psi)} \tag{A.5}$$

Eqn. (A.5) can be evaluated as two separate sums. The derivation of the closed form of the first sum is shown below. An identical procedure is used to find the closed form of the second sum. The first sum is

$$X_{T,1}(e^{j2\pi f}) = \frac{e^{j\psi}}{2} \sum_{k=0}^{N-1} e^{j2\pi k T_s (f_1 - f)}. \tag{A.6}$$

Rewriting eqn. (A.6) as the difference of two sums gives,

$$X_{T,1}(e^{j2\pi f}) = \frac{e^{j\psi}}{2} \left[\sum_{k=0}^{\infty} e^{j2\pi k T_s (f_1 - f)} - \sum_{k=N}^{\infty} e^{j2\pi k T_s (f_1 - f)} \right]. \tag{A.7}$$

If the summations are evaluated, the result is

$$X_{T,1}(e^{j2\pi f}) = \frac{e^{j\psi}}{2} \left[1 + e^{j2\pi T_s (f_1 - f)} + e^{j\psi \pi T_s (f_1 - f)} + \ldots\right] - \frac{e^{j\psi}}{2} \left[e^{j2\pi N T_s (f_1 - f)} + e^{j2\pi (N\ 1) T_s (f_1 - f)} + e^{j2\pi (N\ 2) T_s (f_1 - f)} + \ldots\right]. \tag{A.8}$$

Using the relation

$$\frac{1}{1-x} = 1 + x + x^2 + \ldots \tag{A.9}$$

eqn. (A.8) reduces to

$$X_{T,1}(e^{j2\pi f}) = \frac{e^{j\psi}}{2} \left[\frac{1}{1 - e^{j\pi T_s (f_1 - f)}}\right] - \frac{e^{j\psi}}{2} \left[\frac{e^{j2N\pi T_s (f_1 - f)}}{1 - e^{j\pi T_s (f_1 - f)}}\right]. \tag{A.10}$$

Further simplification by bringing this equation over a common denominator and dividing an exponential term out of both the numerator and denominator yields

$$X_{T,1}(e^{j2\pi f}) = \frac{e^{j\psi} e^{jN\pi T_s(f_1-f)}}{2e^{j\pi T_s(f_1-f)}} \left[\frac{e^{-jN\pi T_s(f_1-f)} - e^{jN\pi T_s(f_1-f)}}{e^{-j\pi T_s(f_1-f)} - e^{j\pi T_s(f_1-f)}}\right]. \quad (A.11)$$

Using the exponential form of the sine function reduces eqn. (A.11) to

$$X_{T,1}(e^{j2\pi f}) = \frac{e^{j(\pi T_s(N-1)(f_1-f)+\psi)}}{2} \left[\frac{sin N\pi T_s(f_1+f)}{sin \pi T_s(f_1-f)}\right]. \quad (A.12)$$

This is the closed form of the first sum in eqn. (A.5). The closed form of the second sum is derived in a similar way and the result is

$$X_{T,2}(e^{j2\pi f}) = \frac{e^{-j(\pi T_s(N-1)(f_1+f)+\psi)}}{2} \left[\frac{sin N\pi T_s(f_1+f)}{sin \pi T_s(f_1+f)}\right]. \quad (A.13)$$

Substituting these two equations into eqn. (A.5) yields the Fourier Transform of eqn. (A.1) as

$$X_T(e^{j2\pi f}) = \frac{e^{-j\pi f T_s(N-1)}}{2} \left[e^{j(\pi f_1 T_s(N-1)+\psi)} \frac{sin N\pi T_s(f_1-f)}{sin \pi T_s(f_1-f)} + e^{-j(\pi f_1 T_s(N-1)+\psi)} \frac{sin N\pi T_s(f_1+f)}{sin \pi T_s(f_1+f)}\right]. \quad (A.14)$$